Effects of ketamine and midazolam on simultaneous EEG/fMRI data during working memory processes

Authors:

Anna E. M. Forsyth*[1], Rebecca McMillan[1], Juergen Dukart[2,3], Jörg F. Hipp[4], & Suresh D. Muthukumaraswamy[1]

*Corresponding Author: Anna Forsyth – afor032@aucklanduni.ac.nz

Affiliations:

1. School of Pharmacy, Faculty of Medical and Health Sciences, The University of Auckland, Private Bag, Auckland, 92019, New Zealand

2. Institute of Neuroscience and Medicine, Brain & Behaviour (INM-7), Research Centre Jülich, Jülich, Germany

3. Institute of Systems Neuroscience, Medical Faculty, Heinrich Heine University Düsseldorf, Düsseldorf, Germany

4. Roche Pharma Research and Early Development, Neuroscience, Opthalmology and Rare Diseases, Roche Innovation Center Basel, Basel Switzerland.

Orcid IDs:

Anna Forsyth: https://orcid.org/0000-0002-3283-2691

Rebecca McMillan: https://orcid.org/0000-0002-4811-5187

Juergen Dukart: https://orcid.org/0000-0003-0492-5644

Jörg F. Hipp: https://orcid.org/0000-0002-7875-2988

Suresh D. Muthukumaraswamy: https://orcid.org/0000-0001-7042-3920

Abstract

Reliable measures of cognitive brain activity from functional neuroimaging techniques may provide early indications of efficacy in clinical trials. Functional magnetic resonance imaging (fMRI) and electroencephalography (EEG) provide complementary spatiotemporal information and simultaneous recording of these two modalities can remove inter-session drug response and environment variability. We sought to assess the effects of ketamine and midazolam on simultaneous electrophysiological and hemodynamic recordings during working memory (WM) processes. Thirty participants were included in a placebo-controlled, three-way crossover design with ketamine and midazolam. Compared to placebo, ketamine administration attenuated theta power increases and alpha power decreases and midazolam attenuated low beta band decreases to increasing WM load. Additionally, ketamine caused larger blood-oxygen-dependent (BOLD) signal increases in the supplementary motor area (SMA) and angular gyrus (AG), and weaker deactivations of the default mode network (DMN), whereas no difference was found between midazolam and placebo. Ketamine administration caused positive temporal correlations between frontal-midline theta (fm-theta) power and the BOLD signal to disappear and attenuated negative correlations. However, the relationship between fm-theta and the BOLD signal from DMN areas was maintained in some participants during ketamine administration, as increasing theta strength was associated with stronger BOLD signal reductions in these areas. The presence of, and ability to manipulate, both positive and negative associations between the BOLD signal and fm-theta suggest the presence of multiple fm-theta components involved in WM processes, with ketamine administration disrupting one or more of these theta-linked WM strategies.

Keywords

'Simultaneous EEG/fMRI', 'Ketamine', 'Midazolam', 'Working Memory', '*n*-back'

Declarations

Conflicts of interest/Competing interests: The authors have no relevant financial or non-financial interests to disclose.

Availability of data and material: Data are available from the corresponding author upon reasonable request. Nifti files of main fMRI result images are available to download at https://doi.org/10.17608/k6.auckland.13726486.v1.

Code availability: Available from the corresponding author upon reasonable request.

Author's contributions:

Anna Forsyth: Conceptualisation, methodology development, data collection, formal analysis, writing and revision of manuscript

Rebecca McMillan: Data collection, revision and editing of manuscript

Juergen Dukart: Conceptualisation, methodology development, revision and editing of manuscript

Jörg F. Hipp: Conceptualisation, methodology development, revision and editing of manuscript

Suresh D. Muthukumaraswamy: Conceptualisation, methodology development, data collection, revision and editing of manuscript

Ethics approval: study was approved by a local Ethics Committee (Central Health and Disability Ethics Committee Ref: 15/CEN/254)). The trial registration can be found at https://www.anzctr.org.au/Trial/Registration/TrialReview.aspx?id=370230.

Consent to participate: Written and informed consent was obtained from all participants.

Consent for publication: Consent obtained from all authors.

Acknowledgements:

Funding: This work was funded by F Hoffman La Roche Ltd.

Introduction

Functional neuroimaging techniques have the potential to provide useful information across all clinical phases of drug development (Borsook et al., 2013). Reliable measures of cognitive brain activity may provide early indications of efficacy, facilitating the development of novel central nervous system (CNS) drugs (Borsook et al., 2013; Musso et al., 2011). fMRI measurements of the BOLD contrast are proving a popular technique for this purpose (Carmichael et al., 2017; Nathan et al., 2014; Wong et al., 2009). BOLD fMRI has excellent spatial specificity and can measure deep cortical structures (Laufs et al., 2003), however, it has limited temporal resolution and as it provides only an indirect measure of brain activity is susceptible to modulation by non-neuronal sources, for example drug-induced changes in vascular tone (Iannetti & Wise, 2007). Conversely, EEG is a direct measure of neural activity with excellent temporal resolution that can quantify brain dynamics (Laufs et al., 2003), however its spatial specificity is limited (Babiloni et al., 2004; Nunez et al., 1994). Together, these two imaging techniques provide complementary spatiotemporal information about the pharmacological modulation of brain function. Simultaneous EEG/fMRI removes participant and/or environment inter-session variability and allows for integration and temporally aligned comparison of the two signal types. We have previously demonstrated the feasibility and utility of simultaneous EEG/fMRI in resting-state pharmacological studies (Forsyth et al., 2018, 2019; McMillan et al., 2019, 2020). Initial research during task-based studies has demonstrated the potential of EEG/fMRI to derive biomarkers sought in drug development studies (Balsters et al., 2011; Diukova et al., 2012; Mobascher et al., 2012; Musso et al., 2011; Warbrick et al., 2012). In the current study we extend our previous resting-state EEG/fMRI pharmacology study (Forsyth et al., 2018, 2019; McMillan et al., 2019, 2020) by using simultaneous EEG/fMRI to study WM processing with the *n*-back task (Kirchner, 1958). Firstly, open questions in the literature about the pharmacological effects on EEG and fMRI signals during WM processing are addressed, followed by a more directed analysis examining whether the integration of simultaneously collected EEG/fMRI signals provides more information than could be obtained from separate recordings.

fMRI has been used to link different brain regions to WM processes indexed with the *n*-back task (for a review see: (Owen et al., 2005)). These studies have demonstrated several cortical areas consistently activated by variants of this task including the lateral premotor cortex, dorsal cingulate and medial premotor cortex, dorsolateral and ventrolateral prefrontal cortex (dlPFC, vlPFC), frontal pole, and medial and lateral posterior parietal cortices. Spatial maps of BOLD signal reductions to increasing WM load resemble the DMN, potentially allowing for maximisation of resources to the activated network (Tomasi et al., 2006). EEG studies have shown that increasing WM load during the *n*-back task is associated with increases in frontal-medial theta (fm-theta) power (4-7 Hz) and modulations to occipital-parietal alpha power (8-13 Hz) (Gundel & Wilson, 1992; Inanaga, 1998; Jensen et al., 2002; Pesonen et al., 2007; Tuladhar et al., 2007). Fm-theta increases have garnered particular attention (Jensen & Tesche, 2002; Sridhar Raghavachari et al., 2001), due in part to the substantial inter-participant variability in this response (for a review see: (Inanaga, 1998)). There is evidence that different local networks engaged by WM tasks independently generate theta activity (Bao & Wu, 2003; Blatow et al., 2003; Flint & Connors, 1996; S. Raghavachari et al., 2006; Silva et al., 1991), and that some fm-theta is driven by hippocampal activity (Alan Gevins et al., 1998; J. M. Hyman et al., 2002; James M. Hyman et al., 2005; Manns et al., 2000; Siapas et al., 2005). A number of studies have attempted to determine the BOLD signal correlates of the modulations to theta power during WM processes utilising separate or simultaneous recordings (for a review, see: (Ahmad et al., 2016)). These studies provide evidence for localisation of the theta power change in the anterior cingulate cortex (ACC) (Esposito et al., 2009), and demonstrate a negative correlation to hemodynamic activity in areas that make up the DMN (Meltzer et al., 2007; Michels et al., 2010; Scheeringa et al., 2008, 2009). The establishment of the fm-theta response as a key electrophysiological signature during WM processing guided the decision to focus on this band during the integration analysis.

This study sought to determine the impact of two previously well-characterised drugs, ketamine and midazolam, on the WM-related neuronal activity, reviewed above, that we measured simultaneously with EEG and fMRI. These two drugs have been shown to modulate WM processes (Adler et al., 1998; Fisher et al., 2006; R. A. E. Honey et al., 2003; Morgan et al., 2004; Rammsayer et al., 2000; Thompson et al., 1999). Midazolam is a positive allosteric modulator of the γ-aminobutyric acid (GABA)-A receptor (Michaloudis et al., 1998; Reinsel et al., 2000), increasing the inhibitory effects of GABA. Inhibition of the GABAergic system has memory facilitating effects (Cruz-Morales et al., 1993), and stimulation results in memory impairment (Izquierdo & Medina, 1991;

Rosat et al., 1992). The impact of midazolam on the BOLD signal during WM processes has not been studied. Indeed, there is limited WM fMRI research on benzodiazepines in general, with just one study assessing the effects of lorazepam during an *n*-back task (Menzies et al., 2007). Midazolam's effects on electrophysiological WM modulations are similarly limited, restricted to the assessment of event-related potentials (ERPs) (Veselis et al., 2009) and EEG signal complexity (Talebi et al., 2012). At subanaesthetic concentrations, ketamine is primarily a non-selective antagonist of the N-Methyl-D-aspartate (NMDA) receptor (Krystal et al., 1994) and has been shown to impair WM processes (Adler et al., 1998; R. A. E. Honey et al., 2003; Morgan et al., 2004). While the impact of ketamine on the BOLD signal during WM processes has been studied (Anticevic et al., 2012a; Compte et al., 2000; Driesen et al., 2013; R. a. E. Honey et al., 2004), its effect on electrophysiology in humans has been limited to assessments of event-related potential (ERP) changes (Ahn et al., 2003; Koychev et al., 2017). However, outside of WM processes, the effect of ketamine on theta band oscillations has been comprehensively studied (Horacek et al., 2010; Lazarewicz et al., 2009; Leuchter et al., 2017; Neymotin et al., 2011; Vlisides et al., 2017; Wang et al., 2018), making it a useful drug to assess whether the analysis of simultaneously recorded EEG/fMRI signals can provide additional information about the fm-theta response.

In summary, we sought to address the above open questions regarding the effects of ketamine and midazolam on electrophysiological oscillatory activity and the effect of midazolam on hemodynamic activity during WM tasks. Furthermore, an assessment of the usefulness of simultaneous EEG/fMRI in a drug study was made, determining if it provided supplementary information to that obtained from separate recordings.

Methods and Methods

Participants and procedure

Thirty male participants aged between 19 and 37 years old (M = 27.3, SD = 6.2), physically and psychologically healthy, with an average body mass index of 24 (SD = 3.5) were recruited and screened for recreational drug use. The recruitment was limited to males due to the changes in GABA levels (Epperson et al., 2002) and EEG metrics (Sumner et al., 2018) across the menstrual cycle, which could confound a repeated-measures design. This study was part of a larger design including resting-state and PCASL recordings and analyses of these have been previously published (Dukart et al., 2018; Forsyth et al., 2018, 2019; McMillan et al., 2019). Participants were scanned on three separate occasions in a placebo-controlled, three-way cross-over design using ketamine, midazolam, and placebo, where the participants were blinded to which drug they were receiving. Participants were randomised using a random-number generator to one of six different condition-order groups. Intravenous access was obtained via a cannula inserted in the antecubital fossa of the left arm. Drugs were administered to a sub-anaesthetic level through an intravenous line controlled by an infusion pump (Alaris PK, UK), programmed by a supervising anaesthesiologist, located in the MR control room. Racemic ketamine was administered with a 0.25 mg/kg bolus dose, followed by a 0.25 mg/kg/hr infusion. Doses were similar to those used in previous literature (Deakin et al., 2008; Muthukumaraswamy et al., 2015). Midazolam was administered with a 0.03 mg/kg bolus dose, followed by a 0.03 mg/kg/hr infusion, resulting in doses similar to prior studies (M. Greicius, 2008; Liang et al., 2015). Collection of plasma would have interfered with our scanning protocol, however information regarding pharmacokinetics and plasma concentrations at similar doses can be found in the literature (for ketamine ~150 ng/mL (Clements & Nimmo, 1981) and for midazolam ~ 20 ng/mL (Platten et al., 1998)). Drug administration commenced 7 minutes into a 16-minute resting-state scan followed by the 9-minute *n*-back task. A high-resolution structural scan was obtained in one of the sessions. There was a minimum of 48 hr between sessions to compensate for the washout periods of each of the drugs. The median inter-sesion interval was 15 days. The drugs were tolerated well, with only minimal and expected side effects, such as nausea and dizziness, in a small number (n = 6) of sessions.

Task procedure

A mirror attached to the MRI head coil reflected a screen outside the scanner upon which were projected the task instructions and stimuli. During this task participants completed eighteen thirty second blocks of two alternating conditions (9 minutes total). The current condition was written above the stimulus on the screen and highlighted in red at the start of each block for two seconds. These blocks then consisted of 14 two second epochs, during which the stimulus was presented for 500 ms. Stimuli were located in the centre of the screen to allow for central fixation, controlling visual artefacts in the EEG. The stimulus consisted of a white arrow on a black screen that

pointed in one of 4 directions (up, down, left, or right) subtending 1° x 0.7° visual angle. Participants held a response box with four buttons with placements that corresponded to the direction of the arrows, resulting in simple spatial mapping from response box to screen. In the first, baseline, condition (0-back) participants were required to press the button that corresponded with the direction of the arrow currently on the screen with their right index finger. They did this for each successive arrow. In the second condition (2-back), participants were required to respond with the button that represented the direction of the arrow that appeared two arrows prior to the one currently on the screen. During the first two arrows of each block of the 2-back condition no response was required. For a schematic of this task, see Figure 1. During screening and on the day of each session prior to scanning participants performed 6 training blocks of the task (3 per condition) outside of the scanner. All participants were able to achieve at least 98% correct for 0-back and 90% correct for 2-back in these training sessions.

Data acquisition

MR images were acquired on a 3 T MR scanner (Siemens Skyra, Erlangen, Germany) with a 20-channel head coil. 246 volumes of BOLD fMRI data were acquired using a T2*-weighted echo planar imaging (EPI) sequence (TR 2200 ms, TE 27 ms, flip angle 79°, 30 interleaved 3 mm slices, voxel size 3 × 3 × 3 mm). In each session, prior to the removal of the EEG cap and its attached contrast markers, a low-resolution Magnetisation-prepared Rapid Gradient-Echo (MPRAGE) scan (TR 1900 ms, TE 3.21 ms, FOV 256 mm^2, flip angle 9°, 96 2 mm slices, voxel size 1.3 × 1.3 × 2.0 mm) was acquired to capture electrode positions. In one of the three sessions for each participant, a high resolution MPRAGE scan was acquired after the EEG cap had been removed to avoid structural distortions ((Klein et al., 2015): TR 2100 ms, TE 3.42 ms, flip angle 9°, 192 slices, voxel size 1 × 1 × 1 mm).

EEG data were recorded continuously using Brain Products (Brain Products GmbH) equipment; two BrainAmp MR plus amplifiers with 64-channel Braincaps. Electrode caps used the manufacturer standard layout with FCz as reference, AFz as ground, and one drop-down electrode attached to the participant's back to record the electrocardiogram (ECG). The amplifier system was placed on a sled behind the head coil within the scanner to reduce cable lengths. Data were recorded with a sampling rate of 5 kHz using BrainVision Recorder software, with BrainVision RecView used to check online data quality during MR acquisition. Filters of 0.1–250 Hz were used, and electrode impedances were below 10 kΩ prior to data acquisition. A SyncBox device (BrainProducts) was used to achieve synchronisation between the EEG hardware and 10 MHz scanner clock. Before entering the scanner, individual electrode placements were recorded using an ultrasound digitisation device (Zebris, Germany) for later source localisation and co-registration. Vitamin E capsules, used as contrast markers, were placed at electrode positions Cz, F5, CP5, and FC6.

fMRI pre-processing

fMRI analyses were carried out using the FMRIB Software Library (FSL) (Jenkinson et al., 2012). The following steps were applied: automated brain extraction using FSL's brain extraction tool (BET; (Smith Stephen M., 2002)), motion correction using MCFLIRT (Jenkinson et al., 2002), spatial smoothing with a Gaussian kernel (5 mm FWHM), high-pass temporal filtering at 0.01 Hz, registration to individual high-resolution structural scans using FLIRT (Jenkinson et al., 2002), and registration to MNI standard brain images using FNIRT (Andersson et al., 2010). Further correction for motion and other physiological artefacts used FSL's FEAT for general linear modelling (GLM) with approximately 50 noise components per dataset derived through Independent Components Analysis (ICA) from FSL's FIX (Griffanti et al., 2014; Salimi-Khorshidi et al., 2014). Due to justified concerns in the pharmacological fMRI field regarding appropriate methods for cleaning physiological noise from the data, a simpler pre-processing pipeline was also run to compare the results to that from ICA de-noising. This included four regressors; average cerebrospinal fluid (CSF) and white matter signals, obtained using masks created by segmenting each individual's high-resolution scan, and their temporal derivatives. Results are presented in Online Resource 2.

EEG Pre-processing

To remove the artefact caused by the fast switching of the MRI gradients, a variant of the standard template removal technique (Allen et al., 2000) was used, where the moving template is compensated for and reset based on obtained fMRI motion parameters (Moosmann et al., 2009). Data were low-pass filtered (100 Hz cut-off frequency) and down-sampled to 500 Hz. The ballistocardiogram artefact caused by the pulsatile motion of blood in the head (Eichele et al., 2010) was removed using an automated method that combines ICA with singular value

decomposition to remove and/or filter components from the data which share high levels of mutual information with the cardiac trace (Liu et al., 2012). The aforementioned steps were performed in EEGLAB (https://sccn.ucsd.edu/wiki/EEGLAB) with subsequent steps performed using a combination of custom scripts and Fieldtrip (Oostenveld et al., 2011). Subsequently, visual inspection of the raw EEG data allowed manual identification and removal of artefacts caused by head motion or jaw clenching. Group mean percentages and their standard errors (brackets) of data removed were as follows: placebo: 0-back = 13.45(1.58), 2-back = 8.58(0.84); ketamine: 0-back = 12.38(1.76), 2-back = 9.94(1.40); midazolam: 0-back = 12.18(2.14), 2-back = 9.31(1.43). Residual artefacts, such as those caused by eye blinks and remaining gradient artefact, were removed using ICA with components manually identified through inspection of temporal and spatial data. On average 2.8/63 (SD = 0.96) components were removed during this step.

Participants that had more than 20% of their EEG data removed during visual inspection and those who had average frame displacements of greater than 0.3 cm in at least 15% of their fMRI volumes were removed from further analysis. The final count of included datasets was 26 for placebo, 24 for ketamine, and 23 for midazolam. As such, when running drug / placebo contrasts, 23 participants had datasets for both ketamine and placebo and 22 for midazolam and placebo.

The following sections outline the main analyses, with the analysis flow depicted in Figure 2.

EEG-alone analysis: spectral modulations and source localisations

Individual electrode positions were co-registered to the structural MRI of each participant. For source modelling, three-shell boundary element models were constructed for each session using brain, skull, and scalp layers (Oostendorp & Oosterom, 1989). EEG data were average-referenced and global covariance matrices were generated for the data, which were filtered into five frequency bands: theta (4-7 Hz), low alpha (8-10 Hz), high alpha (10-13 Hz), low beta (15–26 Hz), and high beta (28–40 Hz). Online Resource 1 describes how these band limits were chosen. Linearly constrained minimum variance beamforming with 5% regularization (Veen et al., 1997) was applied using 8 mm resolution grids warped to the template head-model provided with Fieldtrip to generate spatial filters for each voxel. Power in 0-back and 2-back trials was calculated for each frequency band and at the group level, two-tailed, one-sample *t*-tests were computed using FSL's randomise (Winkler et al., 2014) to correct for multiple comparisons using threshold-free cluster enhancement (TFCE) (Smith & Nichols, 2009) and a defined significance threshold of $p < .025$. The results of these tests were used to mask group average maps to ensure only statistically significant changes were displayed. Additionally, drug versus placebo contrasts were created by performing permuted paired-*t* tests between the task-induced change in power of the drug and placebo maps. There were overlaid on the significant 0 versus 2-back results from the placebo data.

fMRI-alone analysis: BOLD signal modulations

Modulations due to task condition were assessed at the individual level within the same GLM that modelled the noise components. A block design was used to model the BOLD signal during the 18 alternating blocks (9 per condition). The blocks, but not the individual trials, were modelled for subject level analysis. This model was convolved with the gamma hemodynamic response function and added, along with its temporal derivative, to the GLM.

At the group level the task contrast estimates for each drug session were averaged using one-sample *t*-tests, computed using FSL's randomise to correct for multiple comparisons using TFCE and a defined significance threshold of $p < .05$. The results of these tests were used to mask group average maps as with the EEG data. Drug versus placebo contrasts of the task modulations were created by performing permuted paired-*t* tests between the task contrast estimates of the drug conditions, again with TFCE and a defined significance threshold of $p < .05$. Additionally, a formal contrast between the results of the ICA de-noising and CSF/WM regression pipelines were obtained using the same methods as for the drug versus placebo contrasts and can be found in Online Resource 2.

EEG/fMRI analysis: Temporal correlation

A temporal correlation analysis was performed to assess whether the relationship between EEG power modulations and the BOLD signal during WM processing was modulated by drug administration. To establish if the methods used here could demonstrate a relationship between the electrophysiological and hemodynamic signals, the comprehensively established fm-theta increases during WM (Maurer et al., 2015; Mitchell et al., 2008;

Onton et al., 2005) were used as a frequency of interest and the analysis focused on ketamine-induced modulations, as this drug's effect on theta oscillations has also been extensively studied (Horacek et al., 2010; Lazarewicz et al., 2009; Leuchter et al., 2017; Neymotin et al., 2011; Vlisides et al., 2017; Wang et al., 2018). Once established, future work could assess the extent to which BOLD effects during WM processes are explained by all electrophysiological effects and where the two signals modulate independently. Fm-theta increases exhibit substantial inter-individual variability (Inanaga, 1998) and the current study proved no exception; during the placebo condition 11 datasets showed an increase in fm-theta, 10 showed no increase, and 5 were ambiguous. For those who did show an increase, individual coordinates corresponding to the peak power increase during the 2-back condition were selected and used to construct a virtual sensor from which the power time-series was extracted. For those who did not show clear increases, average *x*, *y*, and *z* coordinates from the group who did show increases were used. Table 1 in Online Resource 3 displays the MNI coordinates used for each participant. The resulting time-series were thresholded to remove values exceeding five standard deviations from the mean. These values, and those missing due to removal after visual inspection of the data during pre-processing, were linearly interpolated. A lowpass Butterworth IIR filter (0.0167 Hz) was applied to the power time-series to focus on slow power changes, equivalent to BOLD signal modulations (McMillan et al., 2019).

The EEG theta time-series were added as individual explanatory variables to the regression models described in the FMRI section above, after being convolved with a double-gamma hemodynamic response function. In this way, step wise regressions that would degrade the linear model solutions were avoided. Group averages were calculated for both drug conditions (ketamine and placebo) via one-sample *t*-tests. *Z* statistic images were thresholded using clusters determined by $Z > 2.3$ and an FWE-corrected cluster significance threshold of $p=.05$ was applied (Worsley, 2001). Drug versus placebo contrasts were performed using paired *t*-tests and thresholded similarly to the group averages. For both the averages and the drug versus placebo contrast, permutation testing was conducted using FSL's randomise to correct for multiple comparisons using TFCE and a defined significance level of $p < .05$.

EEG/fMRI analysis: Comparing strengths of EEG theta power and BOLD signal changes

As discussed previously, EEG-fMRI coupling can only be interpreted indirectly due to the divergent nature of the two signals. As such, this analysis sought to provide additional information about BOLD signal correlates of the fm-theta response by using the strength of this response as a covariate in the fMRI GLM. In this analysis, BOLD signal variance explained by inter-subject variability of the fm-theta response was determined by using all participants in one group. To do this, spheres with a 10 mm radius were created around the individual coordinates described previously and the average EEG theta power change to task from within these spheres for each participant was recorded. These were then used as a covariate at the group level when computing the average BOLD signal changes to task.

Results

Behavioural results

Figure 3 shows the average percentage correct for 0- and 2-back trials in each drug condition. Due to technical issues during data collection, where the response interface box failed to transmit response codes to the stimulus presentation software, only eleven participants who had the response box working correctly for all three sessions were included in this analysis. However, even at this lower sample size, a clear pattern of behavioural effects emerged. A 2 (task condition) x 3 (drug session) repeated-measures ANOVA was performed on these data. The results show no significant interaction effect, however, main effects of both task condition ($F(1, 10) = 15.88$, $p = .003$, $\eta_p^2 = .614$) and drug session ($F(2, 20) = 7.69$, $p = .003$, $\eta_p^2 = .435$) were found. Responses during 0-back trials ($M = 91.99$, $SE = 2.28$) were more often correct than during 2-back trials ($M = 84.43$, $SE = 2.46$). Post-hoc Bonferonni tests on the main effect of drug session showed that performance during the midazolam session ($M = 77.35$, $SE = 4.86$) was significantly poorer than during the placebo ($M = 94.55$, $SE = 2.91$) or ketamine ($M = 92.73$, $SE = 2.30$) sessions. While the loss of the behavioural data in the other 19 participants is a limitation, all participants had substantial practice at this task, both during screening and at the start of each study day. All performed well in these practice sessions, and during the actual data collection responses were recorded for all blocks; it was the timing of these responses that was recorded inaccurately by the software. We cannot exclude

the possibility that a sub-set of these participants were performing poorly during the imaging sessions. However, as the group for whom we have valid data performed as expected and were arguably a random sample (independent of participant characteristics or performance), we have no reason to expect that the results of the rest of the participants would have differed substantially from this sample.

EEG-alone analysis: Spectral modulation

These analyses assessed the direction and strength of changes to electrophysiological spectra when WM load was increased. Grand average results of paired *t*-tests between the source activity from 0- and 2-back conditions are displayed in Figure 4. Decreased power was found in all bands during the 2-back trials compared to 0-back trials, across all drug conditions, with the most prominent decreases occurring globally in the low beta (15-26 Hz) band (fig. 4d). These maps are masked by areas that were significant after randomised group single sample analyses, with thresholded cluster-correction of $p < .05$ (two-tailed). The fm-theta increases that were evident when looking at uncorrected group means (Online Resource 1: fig. 1) were not present after correction, presumably due to a lack of statistical power to discern partial-group effects.

Figure 5 displays the significant drug versus placebo contrasts of these spectral power changes. Results from randomised paired-*t* tests between drug sessions are overlaid on group average results from the placebo condition. When comparing 2-back to 0-back trials, ketamine administration resulted in reduced increases in theta (4-7 Hz) spectral power in the paracingulate gyrus, and reduced decreases in the cuneal cortex, compared to the placebo session (fig. 5a). Additionally, it reduced decreases in high alpha (10-13 Hz) power in the 2-back condition in the cerebellum and lingual gyrus (fig. 5b). Midazolam administration reduced decreases in low beta (15-26 Hz) in the inferior occipital cortex, cerebellum, and precentral gyrus (fig. 5c).

fMRI-alone analysis: BOLD signal modulations

These analyses assessed the direction and strength of changes to the BOLD signal with increasing WM load. In lieu of traditional coordinate tables, the fMRI results can be downloaded from https://doi.org/10.17608/k6.auckland.13726486.v1 to allow researchers to view information from all voxels by using a nifti viewer. Figure 6a-c displays the group average results of the task contrast which are masked by significant results of randomised one-sample *t*-tests for each drug condition. Increasing WM load resulted in broadly similar modulations of activity across drug sessions. Increased signal during 2-back trials was seen in the dlPFC, vlPFC, frontal orbital cortex, anterior cingulate cortex (ACC), and parts of the supramarginal and angular gyri. Decreased signal was seen in areas broadly similar to the DMN (medial prefrontal cortex (mPFC), posterior cingulate cortex (PCC), bilateral occipital cortex), and central areas including the precentral gyrus and bilateral insular cortex. Figure 6d displays the results of the significant BOLD drug versus placebo contrasts. Results from randomised paired-*t* tests between drug sessions are overlaid on group average results from the placebo condition. Ketamine administration caused stronger increases during the 2-back condition than seen in the placebo session in the supramarginal and angular gyri (SMG / AG), and reduced decreases in the precentral gyrus, frontal pole (FP), postcentral gyrus, PCC, and central opercular cortex (COC). There were no significant differences in task-driven BOLD signal modulations between the midazolam and placebo sessions.

EEG/fMRI analysis: Temporal correlation

Next, we considered fm-theta EEG informed fMRI analyses. There was a clear group separation between participants who showed fm-theta increases with increasing WM load and those who did not (for a plot of the regressors to visualise this difference see Online Resource 3: Fig.1). Regressors from participants who had fm-theta increases are strongly positively correlated with the task regressor, so temporal correlations between the EEG theta power envelope and the BOLD signal are likely to result in a similar pattern of activity to the task contrast. Interestingly, the regressors from the group without fm-theta increases negatively correlate with the task regressor during the placebo session. Group average regressor correlations with task are as follows; for placebo with fm-theta: $r = 0.69$, $p < .0001^{-38}$, for placebo without fm-theta: $r = -0.23$, $p < .001$, for ketamine with fm-theta: $r = 0.34$, $p < .001^{-5}$, for ketamine without fm-theta: not significantly correlated.

The results of the temporal correlation between the fm-theta power envelopes and the BOLD signal are shown in Figure 7 which displays one-sample *t*-tests for ketamine and placebo conditions. The placebo results (fig. 7a) showed that above and beyond the variance explained by the task contrast, fm-theta modulations were positively correlated with BOLD activity in the PFC, middle and superior frontal gyrus (FG), precentral gyrus, and bilateral

SMG and AG. Additionally, negative correlations were found in the occipital pole (OP), PCC, frontal orbital cortex, FP, and ACC. The only result that survived permutation testing was the positive correlation in the right superior FG during the placebo condition (not pictured). During the ketamine condition, only negative correlations were observed (fig. 7b). These negative correlations were found in the frontal medial and orbital cortices, ACC, precuneus / PCC, and lateral occipital cortex. None of the ketamine session results survived permutation testing. The lack of results after correction may be due to the inter-participant variability in the fm-theta response, indeed when looking at just those who had no fm-theta increases to task there were very few correlations present in the placebo data, and none in the ketamine data (Online Resource 4: Fig.4).

Figure 8 shows the results of a ketamine versus placebo contrast of the temporal correlation results. The placebo session showed increased positive correlations between EEG theta and the BOLD signal in the right middle FG compared to the ketamine session. This result did not survive permutation testing.

EEG/fMRI analysis: Comparing strengths of EEG theta power and BOLD signal changes

To further explore the relationship between EEG fm-theta power changes and the BOLD signal during WM processes, the strength of the fm-theta power change for each individual was used as a covariate in the fMRI one-sample *t*-test of the task contrast. Figure 9 depicts the results, overlaid on the task contrast. During the placebo session, increasing theta strength across participants was associated with a weaker increase in task activity in the left inferior FG and orbital cortex (fig. 9a). During the ketamine session, increasing theta strength across participants was associated with stronger reductions to task in the PCC, OP, left lateral occipital cortex, and the ACC (fig. 9b). It was also associated with stronger increases to task in the posterior precuneus, and weaker increases in the bilateral inferior FG / orbital cortex and the right middle FG. None of these results survived permutation testing.

Discussion

This study first sought to address open questions regarding the effects of midazolam and ketamine on electrophysiological and hemodynamic data during WM processes. As expected, and consistent with previous literature (A Gevins et al., 1997; Klimesch, 1999; Pesonen et al., 2007), an event-related increase in fm-theta power (Online Resource 1: Fig. 1) and decreases in posterior alpha power and global beta power (fig. 4-1b & c) were seen with increasing WM load during the placebo condition. The fm-theta increase did not survive permutation testing (fig. 4-1a), presumably due to it being driven by a sub-group of participants; indeed high inter-participant fm-theta variability is common during WM processes (Inanaga, 1998). Ketamine administration reduced theta power increases in the cingulate gyrus and mitigated theta and high alpha power decreases in posterior regions (fig. 5a-b). Baseline activity may drive these results as ketamine administration increased theta and decreased alpha powers during resting-state with this dataset (Forsyth et al., 2018). Considering that fm-theta increases and alpha decreases are associated with successful memory performance (Klimesch, 1999), the reduced task-induced electrophysiological modulations in these bands during ketamine administration may underlie the lower accuracy in the 2-back condition compared to placebo (fig. 3). These results represent the first assessment of ketamine's effect on oscillatory EEG activity during WM processes in humans. This study is also the first to assess midazolam's effect on oscillatory EEG activity during WM processes. Midazolam administration mitigated the low beta band decreases in the occipital/parietal cortices (fig. 5c). These results may underlie the poorer accuracy seen in the behavioural results (fig. 3), either through motor or cognitive processing. The beta band has been implicated in both the preparation of the motor response in the motor cortices and the active representation and identification of stimuli during WM tasks (Pesonen et al., 2007).

The fMRI results for the placebo session (fig. 6a) closely resembled previous literature (Owen et al., 2005; Tomasi et al., 2006). Increasing memory load resulted in increased BOLD signal in the dlPFC, vlPFC, frontal orbital cortex, parts of the ACC, and the SMG and AG, and decreased signal in DMN areas. Reduced activity in the DMN during 2-back trials may reflect a reallocation of resources to the task-activated network (Menzies et al., 2007). Ketamine administration resulted in stronger increases in some areas (SMG / AG) and reduced decreases in areas of the DMN (fig. 6d). Superior cognitive performance has been associated with the strength of the correlated BOLD signal activations / deactivations during WM tasks (Menzies et al., 2007), so the strengthening of activations combined with the weakening of deactivations seen here may underlie the poorer behavioural performance compared to placebo. The weaker deactivations of the DMN may be driven by already reduced

baseline activity; in the same sessions during resting-state, ketamine reduced connectivity (Forsyth et al., 2019) and the power of low frequency fluctuations (Forsyth et al., 2018) in these areas. The changes in the DMN reflect the results in Anticevic et al. (2012b), however, unlike that study no attenuation of signal in task-activated regions was found. No difference was found in task-related BOLD signal between the midazolam and placebo sessions. This is surprising considering the clear behavioural differences; participants were significantly less accurate during midazolam administration than during either placebo or ketamine sessions. While this is the first study to assess the effect of midazolam on BOLD signal changes during WM tasks, an *n*-back study utilising a comparable dose of lorazepam found reduced frontoparietal activation and temporal/cingulate deactivation compared to placebo (Menzies et al., 2007). However, that study looked at load effects using both 2- and 3-back trials, which may have strengthened their ability to find differences between the benzodiazepine and placebo sessions.

The present study sought to determine if simultaneous EEG/fMRI recordings result in more information about WM processes than separate sessions. Two analyses were run: temporal correlation between the two signals and an assessment of whether BOLD signal variance can be partially explained by differing strengths of EEG power changes across participants. These analyses were run only on ketamine and placebo, and assessed BOLD signal correlates of only the EEG fm-theta response which has been well described previously in the literature (Jensen & Tesche, 2002; S. Raghavachari et al., 2006). When utilising individual fm-theta time courses to discern correlated BOLD signal activity, EEG power modulations explained BOLD signal variance beyond that explained by the task contrast (fig. 7). Results during the placebo session (fig. 7a) reflected previous studies (Meltzer et al., 2007; Sammer et al., 2005; Scheeringa et al., 2008) and ketamine administration (fig. 7b) caused the positive correlations) to disappear, and attenuated the negative correlations. Several of the positively correlated areas (frontal, supramarginal, and precentral gyri) were also areas where ketamine differed from placebo in the fMRI-alone analysis (fig. 6d). While ketamine administration did result in a looser relationship between fm-theta modulation and task than during placebo (Online Resource 3: Fig. 1), they remained strongly correlated, with most 2-back trials eliciting an increase in theta power. Therefore, the loss of positive correlations under ketamine may indicate the existence of multiple independently generated cortical theta rhythms (Bao & Wu, 2003; Blatow et al., 2003; Flint & Connors, 1996; S. Raghavachari et al., 2006; Silva et al., 1991), only some of which are attenuated by NMDA antagonism. As mentioned previously, there are several lines of evidence for independently generated cortical theta rhythm (Bao & Wu, 2003; Blatow et al., 2003; Flint & Connors, 1996; S. Raghavachari et al., 2006; Silva et al., 1991). Furthermore, the *n*-back task is known to involve multiple component processes and disentanglement of these is further confounded by the overlap between encoding and retrieval phases (Esposito et al., 2009).

Another method to explore the EEG/fMRI relationship exploits the inter-participant variability of the fm-theta response (Meltzer et al., 2007), to test whether relative theta strength corresponds to the strength of BOLD signal changes. In the ketamine condition, increasing theta strength was associated with stronger BOLD signal reductions to task in the multiple areas (fig. 9b), similar to non-pharmacological findings with separately recorded data (2007). Additionally, increasing theta strength was related to weaker increases to task in the IFG / orbital cortex. All these areas were found to be negatively correlated between modalities in the temporal correlation analysis. During placebo, the strength of fm-theta changes was only associated with weaker increases in the frontal inferior gyrus / orbital cortex. This contrasts with Meltzer et al.'s results (2007), however potentially the relative ease of the *n*-task compared to the Sternberg task allowed participants to utilise different cognitive strategies during the placebo condition. This confluence of fm-theta components may have reduced the power to discern a relationship between the strength of the changes in each component to the magnitude of the BOLD signal changes. In this scenario, the administration of ketamine disrupted some of these WM processes and this, combined with the comparatively weaker deactivations of DMN areas, allowed a more variable response across the group for the fm-theta / DMN circuit, supplying the statistical power needed to find a relationship between the strength of the changes in each modality. It has been argued that the high inter-participant variance of both DMN inhibition (M. D. Greicius & Menon, 2004) and theta power increases could be evidence of a neurocognitive system that is not essential for task performance in all participants (Meltzer et al., 2007).

Overall, results from the two analyses requiring simultaneous collection of EEG/fMRI suggest ketamine administration disrupts some theta-linked WM strategies, whilst leaving the fm-theta / DMN circuit intact for those who would normally recruit it. As analyses on the EEG signal alone only showed that ketamine reduced fm-theta power (fig. 5), and differences found when analysing the fMRI signal alone (fig. 6d) did not include areas in the DMN, simultaneous acquisition and analysis allowed increased understanding of ketamine-induced modulations to WM processes.

The use of the *n*-back task removed the ability to separately consider different phases of WM processes, such as encoding and retrieval. Future research using a different task with multiple difficulty levels could ascertain whether the differences between the drugs and placebo become stronger and clearer under increasing WM load, and whether they are restricted to certain phases of the WM process. Additionally, for clarity and to utilise the inter-participant variability of the fm-theta response, this study was limited to an assessment of the relationship between fm-theta and the BOLD signal under ketamine administration. Future work could attempt to disentangle pharmacological effects on the electrophysiological and BOLD measurements, for example determining the proportion of BOLD signal modulation explained by the combined effects of all EEG bands.

In conclusion, this is the first study to assess the effects of both ketamine and midazolam on oscillatory activity, and midazolam on BOLD signal changes during WM in humans. The relationship between EEG and fMRI data was assessed using two methodologies that either relied or benefited from simultaneous recording. The combined results revealed a dissociation between ketamine and placebo of the relationship between fm-theta power modulations and BOLD signal changes. These results demonstrate that the combined analysis of simultaneously recorded EEG/fMRI signals yielded information which could not be discerned by separate EEG and fMRI recordings.

References

Adler, CalebM., Goldberg, TerryE., Malhotra, AnilK., Pickar, D., & Breier, A. (1998). Effects of Ketamine on Thought Disorder, Working Memory, and Semantic Memory in Healthy Volunteers. *Biological Psychiatry*, *43*(11), 811–816. https://doi.org/10.1016/S0006-3223(97)00556-8

Ahmad, R. F., Malik, A. S., Kamel, N., Reza, F., & Abdullah, J. M. (2016). Simultaneous EEG-fMRI for working memory of the human brain. *Australasian Physical & Engineering Sciences in Medicine*, *39*(2), 363–378. https://doi.org/10.1007/s13246-016-0438-x

Ahn, K.-H., Youn, T., Cho, S. S., Ha, T. H., Ha, K. S., Kim, M.-S., & Kwon, J. S. (2003). N-Methyl-d-aspartate receptor in working memory impairments in schizophrenia: Event-related potential study of late stage of working memory process. *Progress in Neuro-Psychopharmacology and Biological Psychiatry*, *27*(6), 993–999. https://doi.org/10.1016/S0278-5846(03)00159-3

Allen, P. J., Josephs, O., & Turner, R. (2000). A method for removing imaging artifact from continuous EEG recorded during functional MRI. *NeuroImage*, *12*(2), 230–239. https://doi.org/10.1006/nimg.2000.0599

Andersson, J. L. R., Jenkinson, M., & Smith, S. (2010). *Non-linear registration, aka spatial normalisation* (FMRIB Technical Report TR07 JA2).

Anticevic, A., Gancsos, M., Murray, J. D., Repovs, G., Driesen, N. R., Ennis, D. J., Niciu, M. J., Morgan, P. T., Surti, T. S., Bloch, M. H., Ramani, R., Smith, M. A., Wang, X.-J., Krystal, J. H., & Corlett, P. R. (2012a). NMDA receptor function in large-scale anticorrelated neural systems with implications for cognition and schizophrenia. *Proceedings of the National Academy of Sciences*, *109*(41), 16720–16725. https://doi.org/10.1073/pnas.1208494109

Anticevic, A., Gancsos, M., Murray, J. D., Repovs, G., Driesen, N. R., Ennis, D. J., Niciu, M. J., Morgan, P. T., Surti, T. S., Bloch, M. H., Ramani, R., Smith, M. A., Wang, X.-J., Krystal, J. H., & Corlett, P. R. (2012b). NMDA receptor function in large-scale anticorrelated neural systems with implications for cognition and schizophrenia. *Proceedings of the National Academy of Sciences*, *109*(41), 16720–16725. https://doi.org/10.1073/pnas.1208494109

Babiloni, F., Mattia, D., Babiloni, C., Astolfi, L., Salinari, S., Basilisco, A., Rossini, P. M., Marciani, M. G., & Cincotti, F. (2004). Multimodal integration of EEG, MEG and fMRI data for the solution of the neuroimage puzzle. *Magnetic Resonance Imaging*, *22*(10), 1471–1476. https://doi.org/10.1016/j.mri.2004.10.007

Balsters, J. H., O'Connell, R. G., Martin, M. P., Galli, A., Cassidy, S. M., Kilcullen, S. M., Delmonte, S., Brennan, S., Meaney, J. F., Fagan, A. J., Bokde, A. L. W., Upton, N., Lai, R., Laruelle, M., Lawlor, B., & Robertson, I. H. (2011). Donepezil Impairs Memory in Healthy Older Subjects: Behavioural, EEG and Simultaneous EEG/fMRI Biomarkers. *PLOS ONE*, *6*(9), e24126. https://doi.org/10.1371/journal.pone.0024126

Bao, W., & Wu, J.-Y. (2003). Propagating Wave and Irregular Dynamics: Spatiotemporal Patterns of Cholinergic Theta Oscillations in Neocortex In Vitro. *Journal of Neurophysiology*, *90*(1), 333–341. https://doi.org/10.1152/jn.00715.2002

Blatow, M., Rozov, A., Katona, I., Hormuzdi, S. G., Meyer, A. H., Whittington, M. A., Caputi, A., & Monyer, H. (2003). A Novel Network of Multipolar Bursting Interneurons Generates Theta Frequency Oscillations in Neocortex. *Neuron*, *38*(5), 805–817. https://doi.org/10.1016/S0896-6273(03)00300-3

Borsook, D., Becerra, L., & Fava, M. (2013). Use of functional imaging across clinical phases in CNS drug development. *Translational Psychiatry*, *3*(7), e282. https://doi.org/10.1038/tp.2013.43

Carmichael, O., Schwarz, A. J., Chatham, C. H., Scott, D., Turner, J. A., Upadhyay, J., Coimbra, A., Goodman, J. A., Baumgartner, R., English, B. A., Apolzan, J. W., Shankapal, P., & Hawkins, K. R. (2017). The role of fMRI in drug development. *Drug Discovery Today*. https://doi.org/10.1016/j.drudis.2017.11.012

Clements, J. A., & Nimmo, W. S. (1981). Pharmacokinetics and analgesic effect of ketamine in man. *British Journal of Anaesthesia*, *53*(1), 27–30.

Compte, A., Brunel, N., Goldman-Rakic, P. S., & Wang, X.-J. (2000). Synaptic Mechanisms and Network Dynamics Underlying Spatial Working Memory in a Cortical Network Model. *Cerebral Cortex*, *10*(9), 910–923. https://doi.org/10.1093/cercor/10.9.910

Cruz-Morales, S. E., Quirarte, G. L., Diaz del Guante, M. A., & Prado-Alcalá, R. A. (1993). Effects of GABA antagonists on inhibitory avoidance. *Life Sciences*, *53*(16), 1325–1330. https://doi.org/10.1016/0024-3205(93)90578-Q

Deakin, J. F. W., Lees, J., McKie, S., Hallak, J. E. C., Williams, S. R., & Dursun, S. M. (2008). Glutamate and the Neural Basis of the Subjective Effects of Ketamine: A Pharmaco–Magnetic Resonance Imaging Study. *Archives of General Psychiatry*, *65*(2), 154–164. https://doi.org/10.1001/archgenpsychiatry.2007.37

Diukova, A., Ware, J., Smith, J. E., Evans, C. J., Murphy, K., Rogers, P. J., & Wise, R. G. (2012). Separating neural and vascular effects of caffeine using simultaneous EEG–FMRI: Differential effects of caffeine on cognitive and sensorimotor brain responses. *NeuroImage*, *62*(1), 239–249. https://doi.org/10.1016/j.neuroimage.2012.04.041

Driesen, N. R., McCarthy, G., Bhagwagar, Z., Bloch, M. H., Calhoun, V. D., D'Souza, D. C., Gueorguieva, R., He, G., Leung, H.-C., Ramani, R., Anticevic, A., Suckow, R. F., Morgan, P. T., & Krystal, J. H. (2013). The Impact of NMDA Receptor Blockade on Human Working Memory-Related Prefrontal Function and Connectivity. *Neuropsychopharmacology*, *38*(13), 2613. https://doi.org/10.1038/npp.2013.170

Dukart, J., Holiga, Š., Chatham, C., Hawkins, P., Forsyth, A., McMillan, R., Myers, J., Lingford-Hughes, A. R., Nutt, D. J., Merlo-Pich, E., Risterucci, C., Boak, L., Umbricht, D., Schobel, S., Liu, T., Mehta, M. A., Zelaya, F. O., Williams, S. C., Brown, G., … Sambataro, F. (2018). Cerebral blood flow predicts differential neurotransmitter activity. *Scientific Reports*, *8*(1), 1–11. https://doi.org/10.1038/s41598-018-22444-0

Eichele, T., Moosmann, M., Wu, L., Gutberlet, I., & Debener, S. (2010). Removal of MRI artifacts from EEG recordings. In *Simultaneous EEG and fMRI: Recording, Analysis and Application*. https://doi.org/10.1093/acprof:oso/9780195372731.003.0006

Epperson, C. N., Haga, K., Mason, G. F., Sellers, E., Gueorguieva, R., Zhang, W., Weiss, E., Rothman, D. L., & Krystal, J. H. (2002). Cortical γ-Aminobutyric Acid Levels Across the Menstrual Cycle in Healthy Women and Those With Premenstrual Dysphoric Disorder: A Proton Magnetic Resonance Spectroscopy Study. *Archives of General Psychiatry*, *59*(9), 851–858. https://doi.org/10.1001/archpsyc.59.9.851

Esposito, F., Aragri, A., Piccoli, T., Tedeschi, G., Goebel, R., & Di Salle, F. (2009). Distributed analysis of simultaneous EEG-fMRI time-series: Modeling and interpretation issues. *Magnetic Resonance Imaging*, *27*(8), 1120–1130. https://doi.org/10.1016/j.mri.2009.01.007

Fisher, J., Hirshman, E., Henthorn, T., Arndt, J., & Passannante, A. (2006). Midazolam amnesia and short-term/working memory processes. *Consciousness and Cognition*, *15*(1), 54–63. https://doi.org/10.1016/j.concog.2005.03.004

Flint, A. C., & Connors, B. W. (1996). Two types of network oscillations in neocortex mediated by distinct glutamate receptor subtypes and neuronal populations. *Journal of Neurophysiology*, *75*(2), 951–957. https://doi.org/10.1152/jn.1996.75.2.951

Forsyth, A., McMillan, R., Campbell, D., Malpas, G., Maxwell, E., Sleigh, J., Dukart, J., Hipp, J. F., & Muthukumaraswamy, S. D. (2018). Comparison of local spectral modulation, and temporal correlation, of simultaneously recorded EEG/fMRI signals during ketamine and midazolam sedation. *Psychopharmacology*, *235*(12), 3479–3493. https://doi.org/10.1007/s00213-018-5064-8

Forsyth, A., McMillan, R., Campbell, D., Malpas, G., Maxwell, E., Sleigh, J., Dukart, J., Hipp, J., & Muthukumaraswamy, S. D. (2019). Modulation of simultaneously collected hemodynamic and electrophysiological functional connectivity by ketamine and midazolam. *Human Brain Mapping*, *n/a*(n/a). https://doi.org/10.1002/hbm.24889

Gevins, A, Smith, M. E., McEvoy, L., & Yu, D. (1997). High-resolution EEG mapping of cortical activation related to working memory: Effects of task difficulty, type of processing, and practice. *Cerebral Cortex*, *7*(4), 374–385. https://doi.org/10.1093/cercor/7.4.374

Gevins, Alan, Smith, M. E., Leong, H., McEvoy, L., Whitfield, S., Du, R., & Rush, G. (1998). Monitoring Working Memory Load during Computer-Based Tasks with EEG Pattern Recognition Methods. *Human Factors*, *40*(1), 79–91. https://doi.org/10.1518/001872098779480578

Greicius, M. (2008). Resting-state functional connectivity in neuropsychiatric disorders: *Current Opinion in Neurology*, *24*(4), 424–430. https://doi.org/10.1097/WCO.0b013e328306f2c5

Greicius, M. D., & Menon, V. (2004). Default-Mode Activity during a Passive Sensory Task: Uncoupled from Deactivation but Impacting Activation. *Journal of Cognitive Neuroscience*, *16*(9), 1484–1492. https://doi.org/10.1162/0898929042568532

Griffanti, L., Salimi-Khorshidi, G., Beckmann, C. F., Auerbach, E. J., Douaud, G., Sexton, C. E., Zsoldos, E., Ebmeier, K. P., Filippini, N., Mackay, C. E., Moeller, S., Xu, J., Yacoub, E., Baselli, G., Ugurbil, K.,

Miller, K. L., & Smith, S. M. (2014). ICA-based artefact removal and accelerated fMRI acquisition for improved resting state network imaging. *NeuroImage*, *95*, 232–247. https://doi.org/10.1016/j.neuroimage.2014.03.034

Gundel, A., & Wilson, G. F. (1992). Topographical changes in the ongoing EEG related to the difficulty of mental tasks. *Brain Topography*, *5*(1), 17–25. https://doi.org/10.1007/BF01129966

Honey, R. a. E., Honey, G. D., O'Loughlin, C., Sharar, S. R., Kumaran, D., Bullmore, E. T., Menon, D. K., Donovan, T., Lupson, V. C., Bisbrown-Chippendale, R., & Fletcher, P. C. (2004). Acute Ketamine Administration Alters the Brain Responses to Executive Demands in a Verbal Working Memory Task: An fMRI Study. *Neuropsychopharmacology*, *29*(6), 1203–1214. https://doi.org/10.1038/sj.npp.1300438

Honey, R. A. E., Turner, D. C., Honey, G. D., Sharar, S. R., Kumaran, D., Pomarol-Clotet, E., McKenna, P., Sahakian, B. J., Robbins, T. W., & Fletcher, P. C. (2003). Subdissociative Dose Ketamine Produces a Deficit in Manipulation but not Maintenance of the Contents of Working Memory. *Neuropsychopharmacology*, *28*(11), 2037–2044. https://doi.org/10.1038/sj.npp.1300272

Horacek, J., Brunovsky, M., Novak, T., Tislerova, B., Palenicek, T., Bubenikova-Valesova, V., Spaniel, F., Koprivova, J., Mohr, P., Balikova, M., & Hoschl, C. (2010). Subanesthetic dose of ketamine decreases prefrontal theta cordance in healthy volunteers: Implications for antidepressant effect. *Psychological Medicine*, *40*(9), 1443–1451. https://doi.org/10.1017/S0033291709991619

Hyman, J. M., Wyble, B. P., Rossi, C. A., & Hasselmo, M. E. (2002). Coherence between theta rhythm in rat medial prefrontal cortex and hippocampus. *Abstr Soc Neurosci*, *28*.

Hyman, James M., Zilli, E. A., Paley, A. M., & Hasselmo, M. E. (2005). Medial prefrontal cortex cells show dynamic modulation with the hippocampal theta rhythm dependent on behavior. *Hippocampus*, *15*(6), 739–749. https://doi.org/10.1002/hipo.20106

Iannetti, G. D., & Wise, R. G. (2007). BOLD functional MRI in disease and pharmacological studies: Room for improvement? *Magnetic Resonance Imaging*, *25*(6), 978–988. https://doi.org/10.1016/j.mri.2007.03.018

Inanaga, K. (1998). Frontal midline theta rhythm and mental activity. *Psychiatry and Clinical Neurosciences*, *52*(6), 555–566. https://doi.org/10.1046/j.1440-1819.1998.00452.x

Izquierdo, I., & Medina, J. H. (1991). GABAA receptor modulation of memory: The role of endogenous benzodiazepines. *Trends in Pharmacological Sciences*, *12*, 260–265. https://doi.org/10.1016/0165-6147(91)90567-C

Jenkinson, M., Bannister, P., Brady, M., & Smith, S. (2002). Improved Optimization for the Robust and Accurate Linear Registration and Motion Correction of Brain Images. *NeuroImage*, *17*(2), 825–841. https://doi.org/10.1006/nimg.2002.1132

Jenkinson, M., Beckmann, C. F., Behrens, T. E. J., Woolrich, M. W., & Smith, S. M. (2012). FSL. *NeuroImage*, *62*(2), 782–790. https://doi.org/10.1016/j.neuroimage.2011.09.015

Jensen, O., Gelfand, J., Kounios, J., & Lisman, J. E. (2002). Oscillations in the Alpha Band (9–12 Hz) Increase with Memory Load during Retention in a Short-term Memory Task. *Cerebral Cortex*, *12*(8), 877–882. https://doi.org/10.1093/cercor/12.8.877

Jensen, O., & Tesche, C. D. (2002). Frontal theta activity in humans increases with memory load in a working memory task. *European Journal of Neuroscience*, *15*(8), 1395–1399. https://doi.org/10.1046/j.1460-9568.2002.01975.x

Kirchner, W. K. (1958). Age differences in short-term retention of rapidly changing information. *Journal of Experimental Psychology*, *55*(4), 352–358. https://doi.org/10.1037/h0043688

Klein, C., Hänggi, J., Luechinger, R., & Jäncke, L. (2015). MRI with and without a high-density EEG cap—What makes the difference? *NeuroImage*, *106*, 189–197. https://doi.org/10.1016/j.neuroimage.2014.11.053

Klimesch, W. (1999). EEG alpha and theta oscillations reflect cognitive and memory performance: A review and analysis. *Brain Research Reviews*, *29*(2), 169–195. https://doi.org/10.1016/S0165-0173(98)00056-3

Koychev, I., William Deakin, J. F., El-Deredy, W., & Haenschel, C. (2017). Effects of Acute Ketamine Infusion on Visual Working Memory: Event-Related Potentials. *Biological Psychiatry: Cognitive Neuroscience and Neuroimaging*, *2*(3), 253–262. https://doi.org/10.1016/j.bpsc.2016.09.008

Krystal, J. H., Karper, L. P., Seibyl, J. P., Freeman, G. K., Delaney, R., Bremner, J. D., Heninger, G. R., Bowers, M. B., & Charney, D. S. (1994). Subanesthetic Effects of the Noncompetitive NMDA Antagonist, Ketamine, in Humans: Psychotomimetic, Perceptual, Cognitive, and Neuroendocrine Responses. *Archives of General Psychiatry*, *51*(3), 199–214. https://doi.org/10.1001/archpsyc.1994.03950030035004

Laufs, H., Krakow, K., Sterzer, P., Eger, E., Beyerle, A., Salek-Haddadi, A., & Kleinschmidt, A. (2003). Electroencephalographic signatures of attentional and cognitive default modes in spontaneous brain activity fluctuations at rest. *Proceedings of the National Academy of Sciences*, *100*(19), 11053–11058. https://doi.org/10.1073/pnas.1831638100

Lazarewicz, M. T., Ehrlichman, R. S., Maxwell, C. R., Gandal, M. J., Finkel, L. H., & Siegel, S. J. (2009). Ketamine Modulates Theta and Gamma Oscillations. *Journal of Cognitive Neuroscience*, *22*(7), 1452–1464. https://doi.org/10.1162/jocn.2009.21305

Leuchter, A. F., Espinoza, R., Suthana, N., Hunter, A., & Cook, I. A. (2017). Synergistic effects of ketamine and theta burst stimulation in the treatment of major depressive disorder (MDD). *Brain Stimulation: Basic, Translational, and Clinical Research in Neuromodulation*, *10*(2), 492. https://doi.org/10.1016/j.brs.2017.01.438

Liang, P., Zhang, H., Xu, Y., Jia, W., Zang, Y., & Li, K. (2015). Disruption of cortical integration during midazolam-induced light sedation. *Human Brain Mapping*, *36*(11), 4247–4261. https://doi.org/10.1002/hbm.22914

Liu, Z., de Zwart, J. A., van Gelderen, P., Kuo, L.-W., & Duyn, J. H. (2012). Statistical feature extraction for artifact removal from concurrent fMRI-EEG recordings. *NeuroImage*, *59*(3), 2073–2087. https://doi.org/10.1016/j.neuroimage.2011.10.042

Manns, I. D., Alonso, A., & Jones, B. E. (2000). Discharge Profiles of Juxtacellularly Labeled and Immunohistochemically Identified GABAergic Basal Forebrain Neurons Recorded in Association with the Electroencephalogram in Anesthetized Rats. *The Journal of Neuroscience*, *20*(24), 9252. https://doi.org/10.1523/JNEUROSCI.20-24-09252.2000

Maurer, U., Brem, S., Liechti, M., Maurizio, S., Michels, L., & Brandeis, D. (2015). Frontal Midline Theta Reflects Individual Task Performance in a Working Memory Task. *Brain Topography*, *28*(1), 127–134. https://doi.org/10.1007/s10548-014-0361-y

McMillan, R., Forsyth, A., Campbell, D., Malpas, G., Maxwell, E., Dukart, J., Hipp, J. F., & Muthukumaraswamy, S. (2019). Temporal dynamics of the pharmacological MRI response to subanaesthetic ketamine in healthy volunteers: A simultaneous EEG/fMRI study. *Journal of Psychopharmacology*, *33*(2), 219–229. https://doi.org/10.1177/0269881118822263

McMillan, R., Sumner, R., Forsyth, A., Campbell, D., Malpas, G., Maxwell, E., Deng, C., Hay, J., Ponton, R., Sundram, F., & Muthukumaraswamy, S. (2020). Simultaneous EEG/fMRI recorded during ketamine

infusion in patients with major depressive disorder. *Progress in Neuro-Psychopharmacology and Biological Psychiatry*, *99*, 109838. https://doi.org/10.1016/j.pnpbp.2019.109838

Meltzer, J. A., Negishi, M., Mayes, L. C., & Constable, R. T. (2007). Individual differences in EEG theta and alpha dynamics during working memory correlate with fMRI responses across subjects. *Clinical Neurophysiology*, *118*(11), 2419–2436. https://doi.org/10.1016/j.clinph.2007.07.023

Menzies, L., Ooi, C., Kamath, S., Suckling, J., McKenna, P., Fletcher, P., Bullmore, E., & Stephenson, C. (2007). Effects of γ-Aminobutyric Acid–Modulating Drugs on Working Memory and Brain Function in Patients With Schizophrenia. *Archives of General Psychiatry*, *64*(2), 156–167. https://doi.org/10.1001/archpsyc.64.2.156

Michaloudis, D., Kochiadakis, G., Georgopoulou, G., Fraidakis, O., Chlouverakis, G., Petrou, A., & Pollard, B. J. (1998). The influence of premedication on heart rate variability. *Anaesthesia*, *53*(5), 446–453. https://doi.org/10.1046/j.1365-2044.1998.00323.x

Michels, L., Bucher, K., Lüchinger, R., Klaver, P., Martin, E., Jeanmonod, D., & Brandeis, D. (2010). Simultaneous EEG-fMRI during a Working Memory Task: Modulations in Low and High Frequency Bands. *PLOS ONE*, *5*(4), e10298. https://doi.org/10.1371/journal.pone.0010298

Mitchell, D. J., McNaughton, N., Flanagan, D., & Kirk, I. J. (2008). Frontal-midline theta from the perspective of hippocampal "theta." *Progress in Neurobiology*, *86*(3), 156–185. https://doi.org/10.1016/j.pneurobio.2008.09.005

Mobascher, A., Warbrick, T., Brinkmeyer, J., Musso, F., Stoecker, T., Jon Shah, N., & Winterer, G. (2012). Nicotine effects on anterior cingulate cortex in schizophrenia and healthy smokers as revealed by EEG-informed fMRI. *Psychiatry Research: Neuroimaging*, *204*(2), 168–177. https://doi.org/10.1016/j.pscychresns.2012.09.005

Moosmann, M., Schönfelder, V. H., Specht, K., Scheeringa, R., Nordby, H., & Hugdahl, K. (2009). Realignment parameter-informed artefact correction for simultaneous EEG-fMRI recordings. *NeuroImage*, *45*(4), 1144–1150. https://doi.org/10.1016/j.neuroimage.2009.01.024

Morgan, C. J. A., Mofeez, A., Brandner, B., Bromley, L., & Curran, H. V. (2004). Acute Effects of Ketamine on Memory Systems and Psychotic Symptoms in Healthy Volunteers. *Neuropsychopharmacology*, *29*(1), 208–218. https://doi.org/10.1038/sj.npp.1300342

Musso, F., Brinkmeyer, J., Ecker, D., London, M. K., Thieme, G., Warbrick, T., Wittsack, H.-J., Saleh, A., Greb, W., de Boer, P., & Winterer, G. (2011). Ketamine effects on brain function—Simultaneous

fMRI/EEG during a visual oddball task. *NeuroImage*, *58*(2), 508–525. https://doi.org/10.1016/j.neuroimage.2011.06.045

Muthukumaraswamy, S. D., Shaw, A. D., Jackson, L. E., Hall, J., Moran, R., & Saxena, N. (2015). Evidence that Subanesthetic Doses of Ketamine Cause Sustained Disruptions of NMDA and AMPA-Mediated Frontoparietal Connectivity in Humans. *Journal of Neuroscience*, *35*(33), 11694–11706. https://doi.org/10.1523/JNEUROSCI.0903-15.2015

Nathan, P. J., Phan, K. L., Harmer, C. J., Mehta, M. A., & Bullmore, E. T. (2014). Increasing pharmacological knowledge about human neurological and psychiatric disorders through functional neuroimaging and its application in drug discovery. *Current Opinion in Pharmacology*, *14*, 54–61. https://doi.org/10.1016/j.coph.2013.11.009

Neymotin, S. A., Lazarewicz, M. T., Sherif, M., Contreras, D., Finkel, L. H., & Lytton, W. W. (2011). Ketamine Disrupts Theta Modulation of Gamma in a Computer Model of Hippocampus. *Journal of Neuroscience*, *31*(32), 11733–11743. https://doi.org/10.1523/JNEUROSCI.0501-11.2011

Nunez, P. L., Silberstein, R. B., Cadusch, P. J., Wijesinghe, R. S., Westdorp, A. F., & Srinivasan, R. (1994). A theoretical and experimental study of high resolution EEG based on surface Laplacians and cortical imaging. *Electroencephalography and Clinical Neurophysiology*, *90*(1), 40–57. https://doi.org/10.1016/0013-4694(94)90112-0

Onton, J., Delorme, A., & Makeig, S. (2005). Frontal midline EEG dynamics during working memory. *NeuroImage*, *27*(2), 341–356. https://doi.org/10.1016/j.neuroimage.2005.04.014

Oostendorp, T. F., & Oosterom, A. van. (1989). Source parameter estimation in inhomogeneous volume conductors of arbitrary shape. *IEEE Transactions on Biomedical Engineering*, *36*(3), 382–391. https://doi.org/10.1109/10.19859

Oostenveld, R., Fries, P., Maris, E., & Schoffelen, J.-M. (2011). *FieldTrip: Open Source Software for Advanced Analysis of MEG, EEG, and Invasive Electrophysiological Data* [Research article]. Computational Intelligence and Neuroscience. https://doi.org/10.1155/2011/156869

Owen, A. M., McMillan, K. M., Laird, A. R., & Bullmore, E. (2005). N-back working memory paradigm: A meta-analysis of normative functional neuroimaging studies. *Human Brain Mapping*, *25*(1), 46–59. https://doi.org/10.1002/hbm.20131

Pesonen, M., Hämäläinen, H., & Krause, C. M. (2007). Brain oscillatory 4–30 Hz responses during a visual n-back memory task with varying memory load. *Brain Research*, *1138*, 171–177. https://doi.org/10.1016/j.brainres.2006.12.076

Platten, H.-P., Schweizer, E., Dilger, K., Mikus, G., & Klotz, U. (1998). Pharmacokinetics and the pharmacodynamic action of midazolam in young and elderly patients undergoing tooth extraction. *Clinical Pharmacology & Therapeutics*, *63*(5), 552–560. https://doi.org/10.1016/S0009-9236(98)90106-0

Raghavachari, S., Lisman, J. E., Tully, M., Madsen, J. R., Bromfield, E. B., & Kahana, M. J. (2006). Theta Oscillations in Human Cortex During a Working-Memory Task: Evidence for Local Generators. *Journal of Neurophysiology*, *95*(3), 1630–1638. https://doi.org/10.1152/jn.00409.2005

Raghavachari, Sridhar, Kahana, M. J., Rizzuto, D. S., Caplan, J. B., Kirschen, M. P., Bourgeois, B., Madsen, J. R., & Lisman, J. E. (2001). Gating of Human Theta Oscillations by a Working Memory Task. *Journal of Neuroscience*, *21*(9), 3175–3183. https://doi.org/10.1523/JNEUROSCI.21-09-03175.2001

Rammsayer, T. H., Rodewald, S., & Groh, D. (2000). Dopamine-antagonistic, anticholinergic, and GABAergic effects on declarative and procedural memory functions. *Cognitive Brain Research*, *9*(1), 61–71. https://doi.org/10.1016/S0926-6410(99)00045-2

Reinsel, R. A., Veselis, R. A., Dnistrian, A. M., Feshchenko, V. A., Beattie, B. J., & Duff, M. R. (2000). Midazolam decreases cerebral blood flow in the left prefrontal cortex in a dose-dependent fashion. *International Journal of Neuropsychopharmacology*, *3*(2), 117–127. https://doi.org/10.1017/S1461145700001814

Rosat, R., Da-Silva, R. C., Zanatta, M. S., Medina, J. H., & Izquierdo, I. (1992). Memory consolidation of a habituation task: Role of N-methyl-D-aspartate, cholinergic muscarinic and GABA-A receptors in different brain regions. - Abstract—Europe PMC. *Brazilian Journal of Medical and Biological Research*, *25*(3), 267–273.

Salimi-Khorshidi, G., Douaud, G., Beckmann, C. F., Glasser, M. F., Griffanti, L., & Smith, S. M. (2014). Automatic denoising of functional MRI data: Combining independent component analysis and hierarchical fusion of classifiers. *NeuroImage*, *90*, 449–468. https://doi.org/10.1016/j.neuroimage.2013.11.046

Sammer, G., Blecker, C., Gebhardt, H., Kirsch, P., Stark, R., & Vaitl, D. (2005). Acquisition of typical EEG waveforms during fMRI: SSVEP, LRP, and frontal theta. *NeuroImage*, *24*(4), 1012–1024. https://doi.org/10.1016/j.neuroimage.2004.10.026

Scheeringa, R., Bastiaansen, M. C. M., Petersson, K. M., Oostenveld, R., Norris, D. G., & Hagoort, P. (2008). Frontal theta EEG activity correlates negatively with the default mode network in resting state. *International Journal of Psychophysiology*, *67*(3), 242–251. https://doi.org/10.1016/j.ijpsycho.2007.05.017

Scheeringa, R., Petersson, K. M., Oostenveld, R., Norris, D. G., Hagoort, P., & Bastiaansen, M. C. M. (2009). Trial-by-trial coupling between EEG and BOLD identifies networks related to alpha and theta EEG power increases during working memory maintenance. *NeuroImage*, *44*(3), 1224–1238. https://doi.org/10.1016/j.neuroimage.2008.08.041

Siapas, A. G., Lubenov, E. V., & Wilson, M. A. (2005). Prefrontal Phase Locking to Hippocampal Theta Oscillations. *Neuron*, *46*(1), 141–151. https://doi.org/10.1016/j.neuron.2005.02.028

Silva, L. R., Amitai, Y., & Connors, B. W. (1991). Intrinsic oscillations of neocortex generated by layer 5 pyramidal neurons. *Science*, *251*(4992), 432–435. https://doi.org/10.1126/science.1824881

Smith, S. M., & Nichols, T. E. (2009). Threshold-free cluster enhancement: Addressing problems of smoothing, threshold dependence and localisation in cluster inference. *NeuroImage*, *44*(1), 83–98. https://doi.org/10.1016/j.neuroimage.2008.03.061

Smith Stephen M. (2002). Fast robust automated brain extraction. *Human Brain Mapping*, *17*(3), 143–155. https://doi.org/10.1002/hbm.10062

Sumner, R. L., McMillan, R. L., Shaw, A. D., Singh, K. D., Sundram, F., & Muthukumaraswamy, S. D. (2018). Peak visual gamma frequency is modified across the healthy menstrual cycle. *Human Brain Mapping*, *39*(8), 3187–3202. https://doi.org/10.1002/hbm.24069

Talebi, N., Nasrabadi, A. M., & Curran, T. (2012). Investigation of changes in EEG complexity during memory retrieval: The effect of midazolam. *Cognitive Neurodynamics*, *6*(6), 537–546. https://doi.org/10.1007/s11571-012-9214-0

Thompson, J. M., Neave, N., Moss, M. C., Scholey, A. B., Wesnes, K., & Girdler, N. M. (1999). Cognitive properties of sedation agents: Comparison of the effects of nitrous oxide and midazolam on memory and mood. *British Dental Journal*, *187*(10), 557–562. https://doi.org/10.1038/sj.bdj.4800330

Tomasi, D., Ernst, T., Caparelli, E. C., & Chang, L. (2006). Common deactivation patterns during working memory and visual attention tasks: An intra-subject fMRI study at 4 Tesla. *Human Brain Mapping*, *27*(8), 694–705. https://doi.org/10.1002/hbm.20211

Tuladhar, A. M., Huurne, N. ter, Schoffelen, J.-M., Maris, E., Oostenveld, R., & Jensen, O. (2007). Parieto-occipital sources account for the increase in alpha activity with working memory load. *Human Brain Mapping*, *28*(8), 785–792. https://doi.org/10.1002/hbm.20306

Veen, B. D. V., Drongelen, W. V., Yuchtman, M., & Suzuki, A. (1997). Localization of brain electrical activity via linearly constrained minimum variance spatial filtering. *IEEE Transactions on Biomedical Engineering*, *44*(9), 867–880. https://doi.org/10.1109/10.623056

Veselis, R. A., Pryor, K. O., Reinsel, R. A., Li, Y., Mehta, M., & Johnson, R. (2009). Propofol and midazolam inhibit conscious memory processes very soon after encoding: An event related potential study of familiarity and recollection in volunteers. *Anesthesiology*, *110*(2), 295–312. https://doi.org/10.1097/ALN.0b013e3181942ef0

Vlisides, P. E., Bel-Bahar, T., Lee, U., Li, D., & Kim, H. (2017). Neurophysiologic correlates of ketamine sedation and anesthesia: A high-density electroencephalography study in healthy volunteers. *Anesthesiology*, *127*, 58–69.

Wang, X., Pinto-Duarte, A., Behrens, M. M., Zhou, X., & Sejnowski, T. J. (2018). Ketamine independently modulated power and phase-coupling of theta oscillations in Sp4 hypomorphic mice. *PLoS ONE*, *13*(3). https://doi.org/10.1371/journal.pone.0193446

Warbrick, T., Mobascher, A., Brinkmeyer, J., Musso, F., Stoecker, T., Shah, N. J., Fink, G. R., & Winterer, G. (2012). Nicotine Effects on Brain Function during a Visual Oddball Task: A Comparison between Conventional and EEG-informed fMRI Analysis. *Journal of Cognitive Neuroscience*, *24*(8), 1682–1694. https://doi.org/10.1162/jocn_a_00236

Winkler, A. M., Ridgway, G. R., Webster, M. A., Smith, S. M., & Nichols, T. E. (2014). Permutation inference for the general linear model. *NeuroImage*, *92*, 381–397. https://doi.org/10.1016/j.neuroimage.2014.01.060

Wong, D. F., Tauscher, J., & Gründer, G. (2009). The Role of Imaging in Proof of Concept for CNS Drug Discovery and Development. *Neuropsychopharmacology*, *34*(1), 187–203. https://doi.org/10.1038/npp.2008.166

Worsley, K. (2001). Statistical analysis of activation images. In *Functional MRI: An Introduction to Methods* (pp. 251–270). Oxford University Press.

Figure Legends

Fig. 1 Schematic of the n-back task used. Stimuli consisted of a centrally positioned arrow pointing in one of four directions (white arrows). Two alternating conditions with durations of 30 seconds per condition were run, 9 times in total. Participants held a response box with four buttons; at the top, bottom, left, and right of the box. During the first condition, 0-back, participants pressed the button that corresponded to the arrow direction on the screen (e.g. if the arrow pointed up, they pressed the bottom at the top of the response box). During the second condition, 2-back, they pressed the button corresponding to the direction of the arrow presented two prior to the one currently on the screen. Correct responses are denoted by black arrows.

Fig 2. Schematic of analysis flow

Fig. 3 Bar chart of behavioural results for the *n*-back task. Due to issues during data collection this bar chart represents the % correct for 0 and 2-back conditions for 11 participants whose responses were logged for all three sessions. Stars denote significance at the $p < .05$ level.

Fig. 4 EEG power spectra changes during increasing working memory load. Grand-averaged statistical parametric maps for the EEG frequency bands (paired *t*-test between 0- and 2-back trials) for the placebo (1), ketamine (2), and midazolam (3) sessions: a. Theta (4-7 Hz), b. Low Alpha (8-10 Hz), c. High Alpha (10-13 Hz), d. Low Beta (15-26 Hz), and e. High Beta (28-40 Hz). All maps are masked by areas which demonstrated significant activity from a randomised group one-sample analysis, with a thresholded cluster-correction of $p < .05$ (two-tailed).

Fig. 5 Differences in task-induced EEG power spectra changes between drug and placebo sessions. Grand-averaged EEG spectral statistical parametric maps of the difference (paired-*t*) between either ketamine or midazolam's task-induced modulations (difference between 0- and 2-back), and those from the placebo condition. These maps are shown on top of the grand-averaged task-induced changes in the placebo condition only, with blue-light blue depicting decreases in power, and red-yellow depicting increases. The overlaid difference paired-*t* test maps are masked by areas which demonstrated significant differences from a randomised paired-*t* analysis between the drugs and placebo, with a thresholded cluster correction of $p < .05$ (two-tailed). Dark-light green depicts areas where drug administration resulted in greater power than placebo, and dark-light pink, where power was greater in placebo. Note: if these are over an area that was reduced in power by increasing memory load, this can be interpreted as this drug causing 'less reduction' in power. Only significant differences between sessions are displayed; a: Ketamine versus placebo contrast in the theta (4-7 Hz) band, b: Ketamine versus placebo contrast in the high alpha (10-13 Hz) band, and c: Midazolam versus placebo contrast in the low beta (15-26 Hz) band.

Fig. 6 fMRI BOLD changes during increasing working memory load for each drug session separately and the difference between ketamine and placebo sessions. (a), (b), & (c) depict grand-averaged statistical parametric maps comparing BOLD signal differences between 0- and 2-back conditions, for each drug session (a. Placebo, b. Ketamine, c. Midazolam). Dark-light blue depicts areas where signal was reduced during the 2-back condition compared to 0-back, and red-yellow areas where signal increased. Maps are masked by areas which demonstrated significant differences from a randomised paired-*t* test, with a thresholded cluster correction of $p < .05$ (two-tailed). Shown in (d) are grand-averaged statistical parametric maps comparing BOLD signal differences between the task-induced modulations (difference between 0- and 2-back) of the ketamine and placebo sessions. These maps are shown on top of the grand-averaged task-induced changes in the placebo condition only. The overlaid difference maps between ketamine and placebo are masked by areas which demonstrated significant differences from a randomised paired *t*-test with a thresholded cluster correction of $p < .05$ (two-tailed). Dark-light green depicts areas where drug administration resulted in increased BOLD signal compared to placebo. Note: if these are over an area where signal was reduced by increasing memory load, this

can be interpreted as the drug causing ‘less reduction’ in BOLD signal. Only significant differences are displayed (no differences were found between midazolam and placebo).

Fig. 7 Temporal correlations between EEG theta power and the BOLD signal. Thresholded (min = 2.3, max = 4) statistical *z*-maps of the positive (red-yellow) and negative (dark-light blue) temporal correlations between the EEG theta (4-7 Hz) power envelope derived from a frontal-medial source and the BOLD signal. Displayed are those the placebo (a) and ketamine (b) sessions.

Fig. 8 Difference between ketamine and placebo sessions of the temporal correlations between EEG theta power and the BOLD signal. Grand-averaged results of a paired-*t* test between ketamine and placebo for the temporal correlations between EEG theta power and the BOLD signal. Dark-light pink displays areas where temporal correlations in the placebo condition were stronger than during the ketamine condition. These are overlaid on thresholded statistical *z*-maps of the positive (red-yellow) and negative (dark-light blue) temporal correlations between the EEG theta (4-7 Hz) power envelope derived from a frontal-medial source and the BOLD signal during the placebo condition only.

Fig. 9 Assessing fMRI variance explained by the strength of changes in fm-theta power. Depicted are the areas where the strength of BOLD signal modulations were associated with the strength of the fm-theta power change for the placebo (A) and ketamine (B) sessions. Areas in dark-light green are those where increasing theta strength across participants was negatively correlated with task-induced BOLD activity, and those in dark-light pink are the positive correlations. These are overlaid on the fMRI group-average results of the task contrast for that session. All results are thresholded *z*-statistical maps (min = 2.3, max = 4).

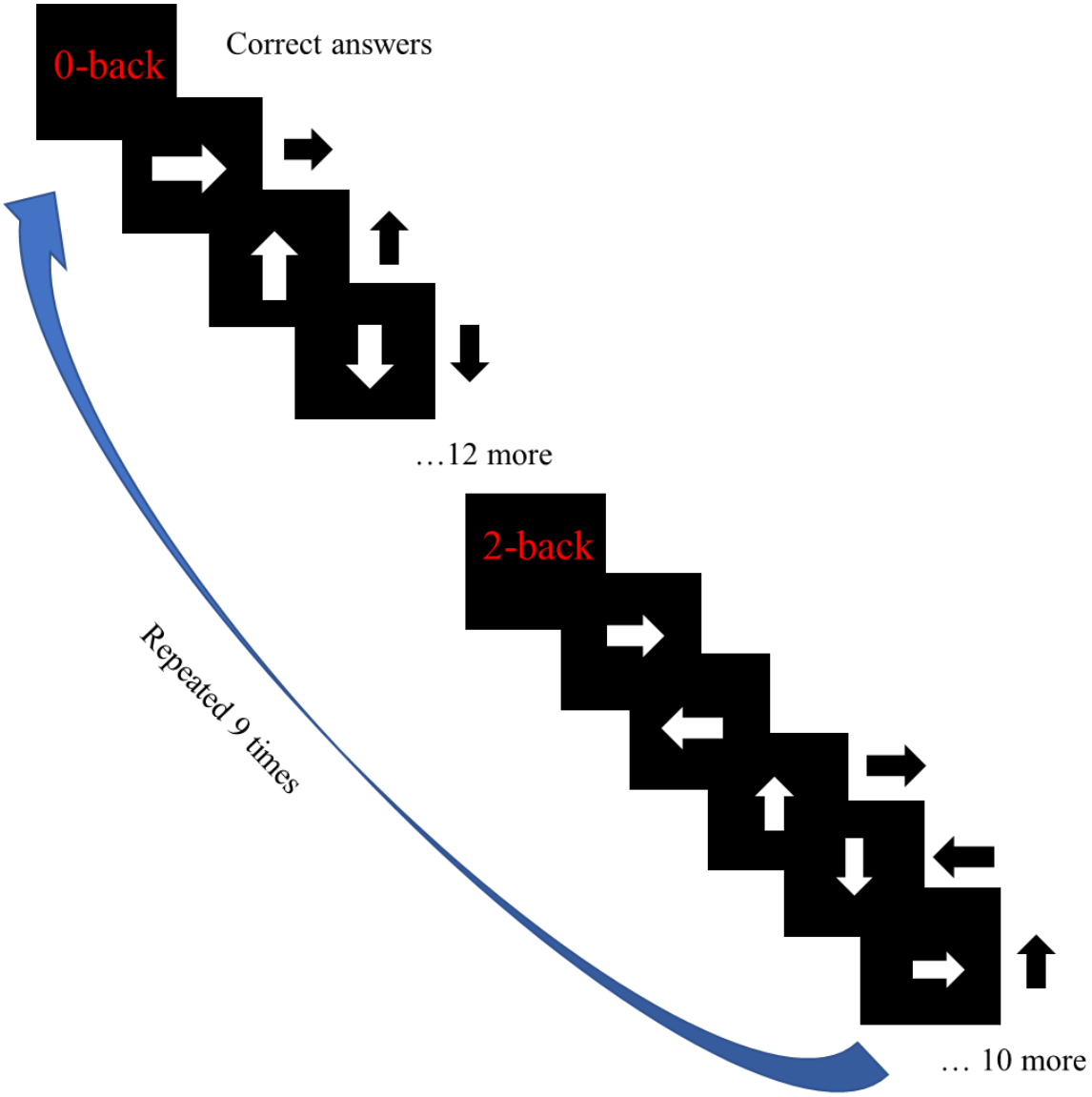
0-back
Correct answers
…12 more
2-back
Repeated 9 times
… 10 more

[Figure 1]

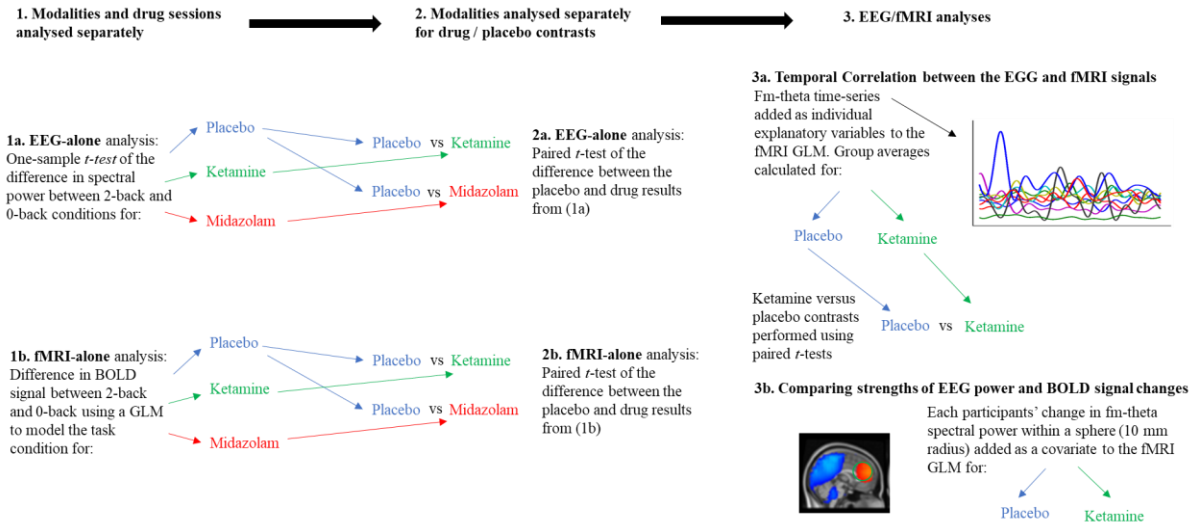
1. Modalities and drug sessions analysed separately
2. Modalities analysed separately for drug / placebo contrasts
3. EEG/fMRI analyses
1a. EEG-alone analysis: One-sample t-test of the difference in spectral power between 2-back and 0-back conditions for:
Placebo
Ketamine
Midazolam
Placebo vs Ketamine
Placebo vs Midazolam
2a. EEG-alone analysis: Paired t-test of the difference between the placebo and drug results from (1a)
1b. fMRI-alone analysis: Difference in BOLD signal between 2-back and 0-back using a GLM to model the task condition for:
Placebo
Ketamine
Midazolam
Placebo vs Ketamine
Placebo vs Midazolam
2b. fMRI-alone analysis: Paired t-test of the difference between the placebo and drug results from (1b)
3a. Temporal Correlation between the EGG and fMRI signals
Fm-theta time-series added as individual explanatory variables to the fMRI GLM. Group averages calculated for:
Placebo
Ketamine
Ketamine versus placebo contrasts performed using paired t-tests
Placebo vs Ketamine
3b. Comparing strengths of EEG power and BOLD signal changes
Each participants' change in fm-theta spectral power within a sphere (10 mm radius) added as a covariate to the fMRI GLM for:
Placebo
Ketamine

[Figure 2]

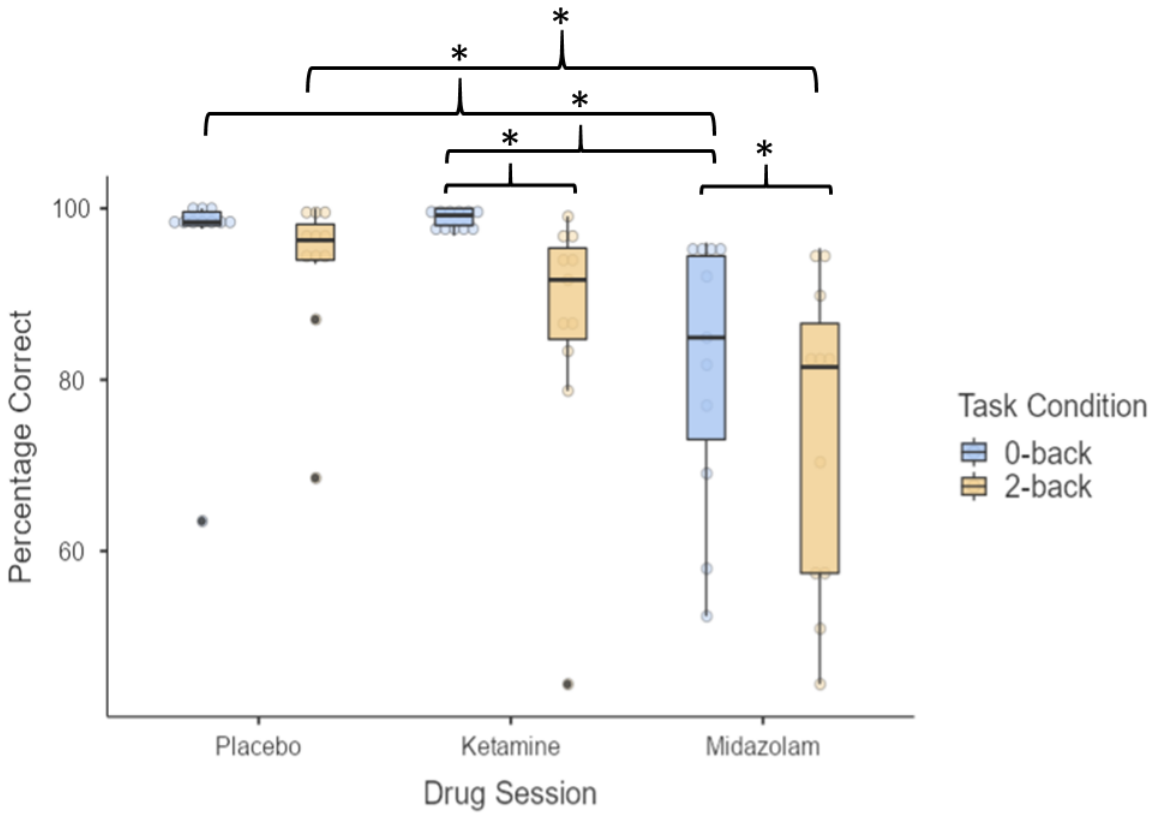
*
*
*
*
*
100
80
60
Percentage Correct
Placebo
Ketamine
Midazolam
Drug Session
Task Condition
0-back
2-back

[Figure 3]

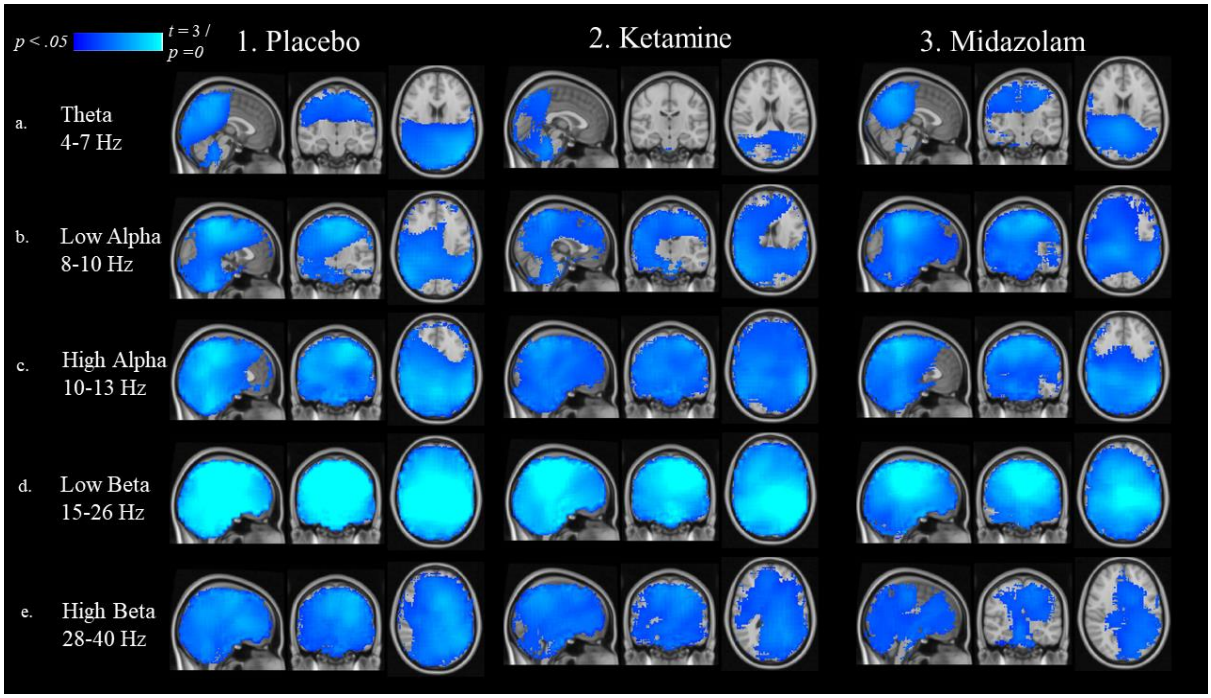
p < .05
t = 3 / p = 0
1. Placebo
2. Ketamine
3. Midazolam
a. Theta 4-7 Hz
b. Low Alpha 8-10 Hz
c. High Alpha 10-13 Hz
d. Low Beta 15-26 Hz
e. High Beta 28-40 Hz

[Figure 4]

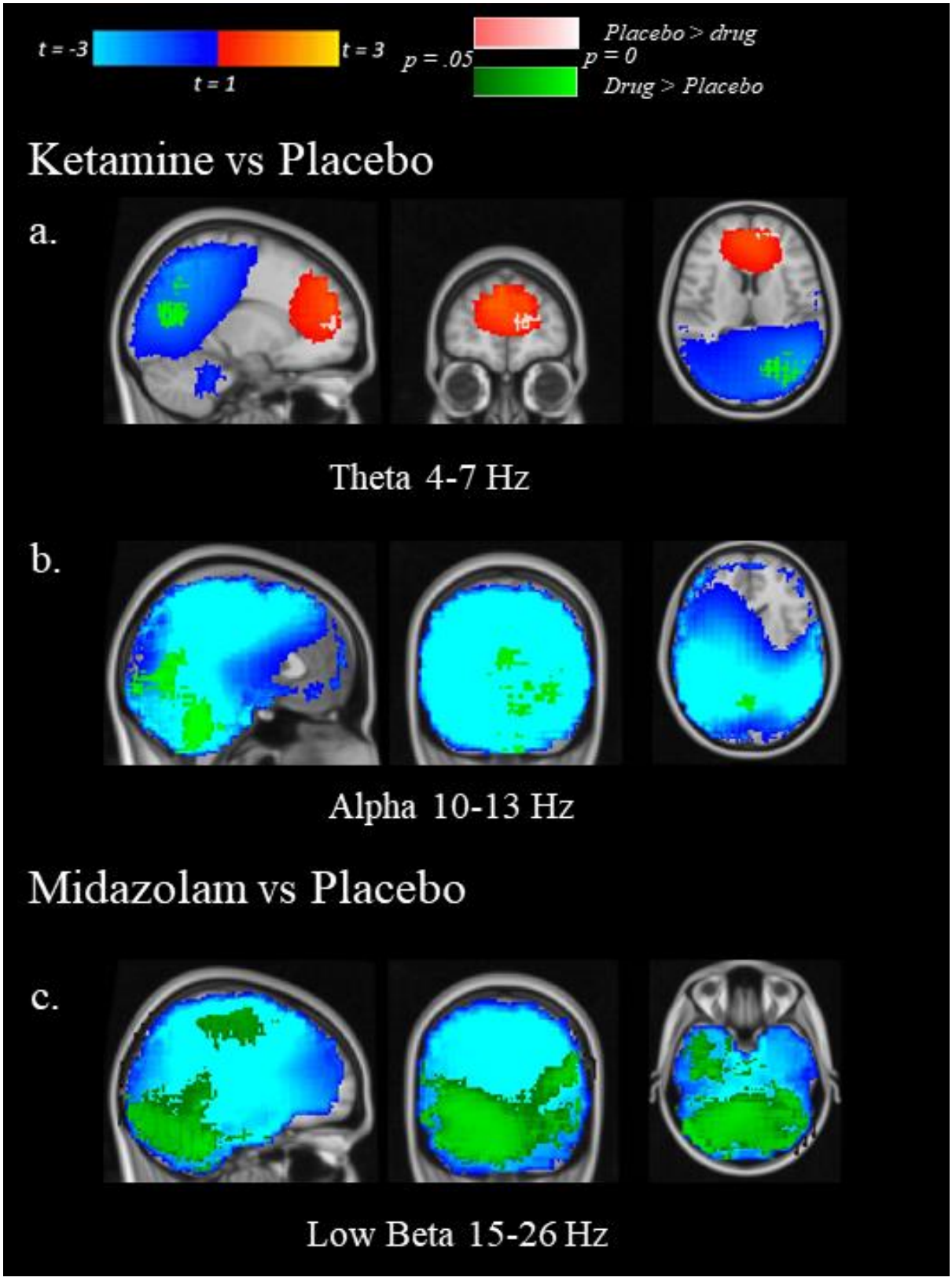
t = -3
t = 3
t = 1
p = .05
Placebo > drug
p = 0
Drug > Placebo
Ketamine vs Placebo
a.
Theta 4-7 Hz
b.
Alpha 10-13 Hz
Midazolam vs Placebo
c.
Low Beta 15-26 Hz

[Figure 5]

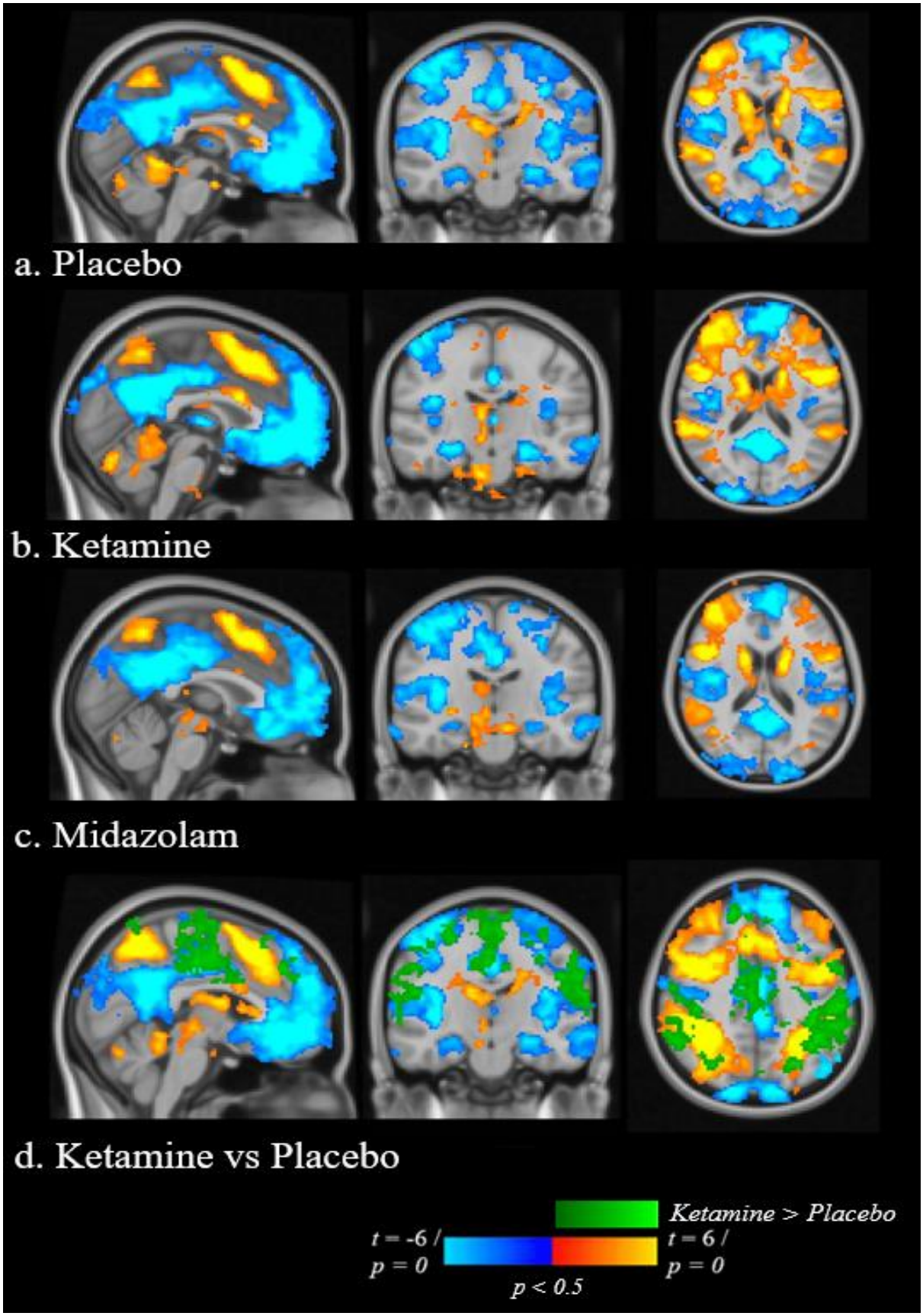
a. Placebo
b. Ketamine
c. Midazolam
d. Ketamine vs Placebo
t = -6 /
p = 0
p < 0.5
Ketamine > Placebo
t = 6 /
p = 0

[Figure 6]

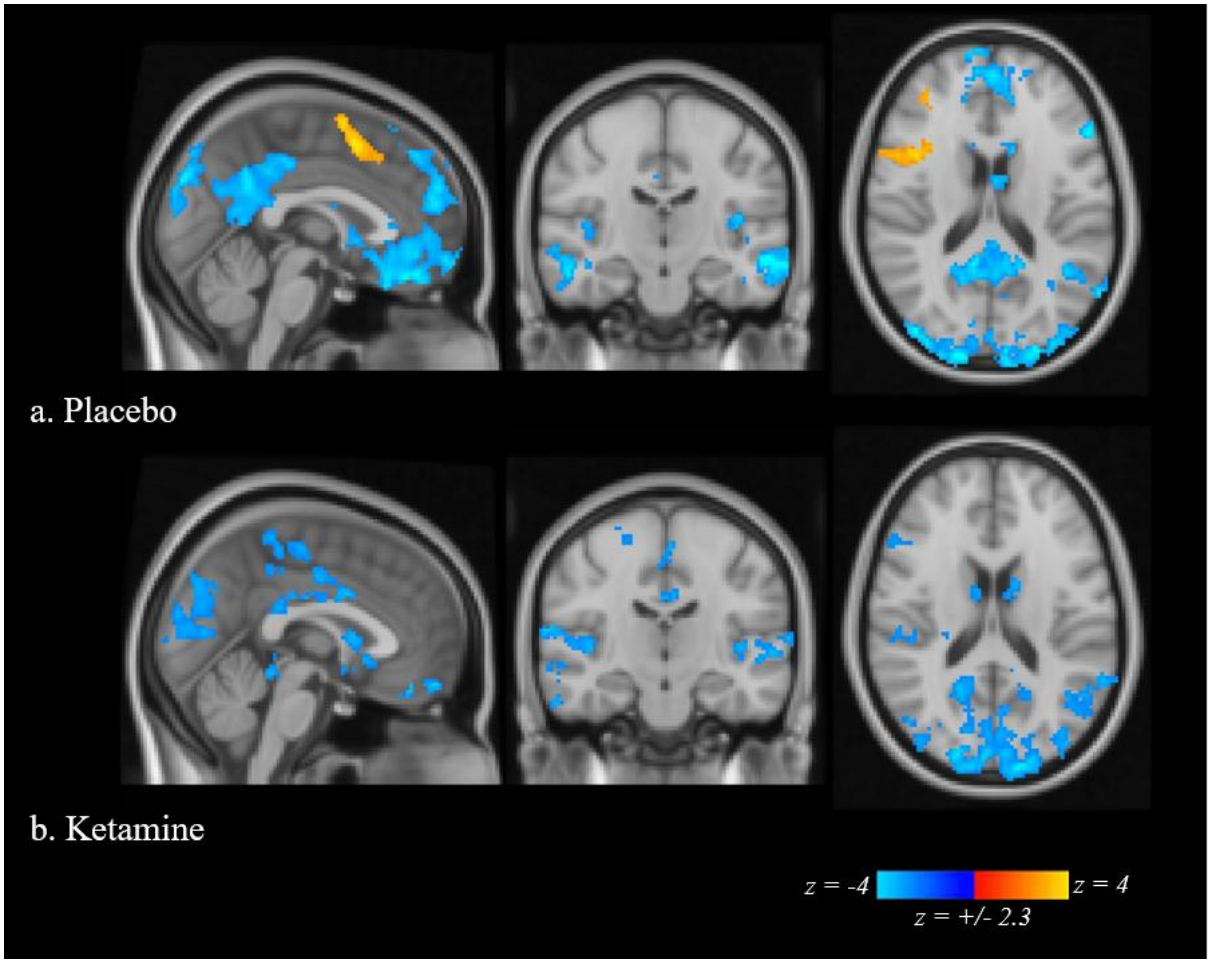

[Figure 7]

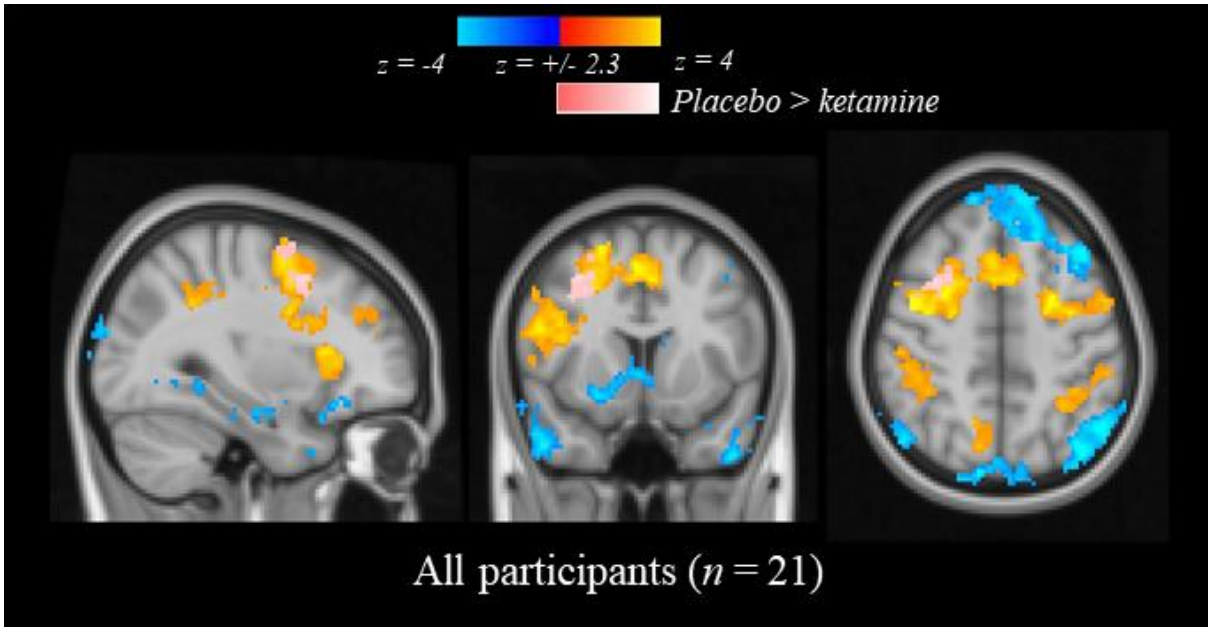

[Figure 8]

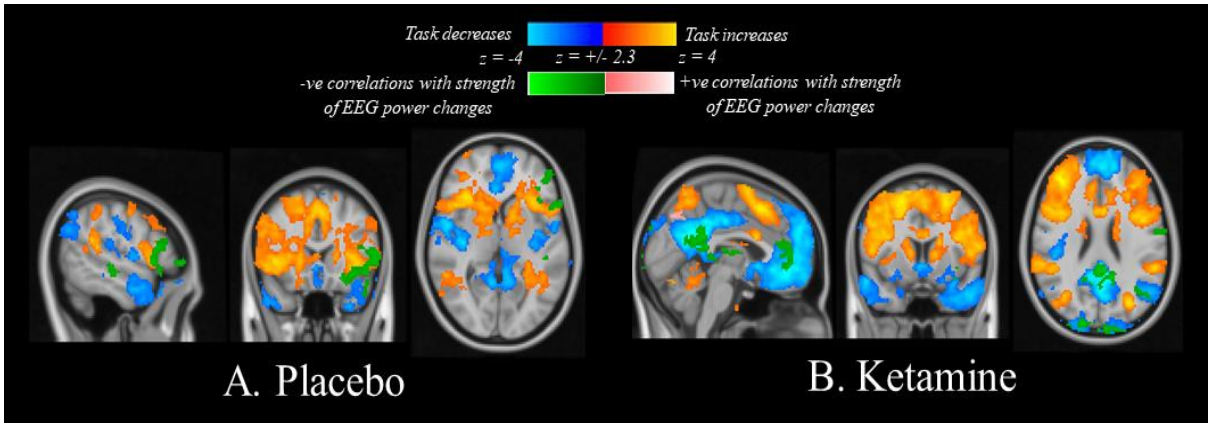
Task decreases
Task increases
z = -4
z = +/- 2.3
z = 4
-ve correlations with strength of EEG power changes
+ve correlations with strength of EEG power changes
A. Placebo
B. Ketamine

[Figure 9]